Reviewer Responses

An Undercurrent off the East Coast of Sri Lanka

Arachaporn Anutaliya et al.

The author comment is presented in the following sequence: (1) itemized comments from the referee in black, (2) author's response in red, (3) author's changes in manuscript in red italic.

Anonymous Referee #1 Received and published: 22 August 2017

1. P4 L1-12. The level of no motion for the calculation of geostrophic velocity is not very clear here. If the level of no motion was picked at 1000 m, where the currents are relatively strong, there would be a bias in the geostrophic calculations. The motion would be more relative and not absolute.
   (2) The velocity from the glider presented in figure 2 is referenced to its depth-averaged velocity, while that in figure 3 is referenced to the surface velocity derived from satellite absolute dynamic topography. Velocities from POP and HYCOM in both figures are total velocity. We have rewritten the text to make this clearer.
   (3) *Clarification has been added to the manuscript (P4, L13-17).*
   "As noted above, geostrophic velocities derived from glider measurements, during March 18-30, 2014 (Figure 2a) and May 28–June 8, 2014 (Figure 2d), are referenced to the depth-averaged velocity measured directly by the gliders. Velocity transects from HYCOM (Figure 2b, e) and POP (Figure 2c, f) were constructed from monthly averages of total velocity in March and June for the periods of 2003-2012 and 1995-2007, respectively."

   Figure caption of Fig. 2 is also revised.
   "Figure 2: Geostrophic meridional velocity referenced to the depth-averaged velocity across 8° N from glider measurements during March 18-30, 2014 (a) and May 24 – Jun 8, 2014 (d), the mean absolute meridional velocity from HYCOM (b and e) and POP (c and f) in March and June over 2003-2012 and 1995-2007 periods, respectively. The black dashed line marks the typical eastern extent of the undercurrent core; the region bounded to its west is used for a subsequent averaging in Figure 3. Thin black lines are plotted every 10 cm s^{-1}, and thick black lines are plotted every 50 cm s^{-1}."

2. Page 4, L2. Though the structures are in good agreement, there are differences in the intensity. For example, the offshore currents are very weak in the model, especially during March.
   (2) The reviewer is correct, the intensity differs between the models and observations, as well as from season to season. The original text was not precise and has been made clearer. We have also added a table that describes the characteristics of the undercurrent in March (Table 1) and June (Table 2).
   (3) *The manuscript has been revised (P4, L19-30).*
   "The model transects show reasonable agreement with that from the gliders in regard to the vertical structure of both the surface current and undercurrent. In March, the core of the observed undercurrent is located about 55 km from the

coast and has a maximum speed of 16-25 cm s^{-1} southward (Table 1). HYCOM and POP have maximum flows in the reverse direction to the surface i.e. southward, at 570 and 268 m, respectively (Figure 2a-b) while glider measurements show maximum subsurface flow at the deepest measured depth of 1000 m (Figure 2c). In June, a northward undercurrent is observed below approximately 250 m with a maximum speed greater than 20 cm s^{-1} at about 900 m (Figure 2d-f; Table 2). The summer undercurrent is approximately 165 km wide in the OGCMs. The velocity section derived from gliders shows a wider undercurrent of 210 km with two cores: a deep core that is approximately 100 km wide centered at 82.2°E and a shallow core at 400 m near 82.75°E (Figure 2d). This double-core feature is also evident in some individual model years, but is not present in the multi-year mean (Figure 2e, f)."

Tables have been added to the manuscript.

	v_{max} (cm s^{-1})	Depth of v_{max} (m)	Position of v_{max} (°E)	Depth of reversal (m)	Width (km)
Glider	-25.3	1000.0	82.06	232.0	107.8
HYCOM	-16.2	570.4	82.00	83.3	151.9
POP	-18.9	268.5	81.95	77.4	209.1

Table 1. Statistics of the undercurrent across 8°N in March from the glider geostrophic velocity as presented in Figure 2 and mean absolute velocity from HYCOM and POP. Here, v_{max} represents maximum meridional velocity; depth of reversal is defined as the depth of the zero meridional velocity at the location of the maximum velocity; width of the undercurrent is defined as the distance from the coast at the depth of maximum velocity to the location where the meridional velocity is zero.

	v_{max} (cm s^{-1})	Depth of v_{max} (m)	Position of v_{max} (°E)	Depth of reversal (m)	Width (km)
Glider	29.6	1000.0	81.90-82.40	117.3-300	206.9
HYCOM	20.6	800.8	82.08	244.8	165.1
POP	27.6	918.4	82.15	244.1	172.8

Table 2. Same as Table 1 but for June.

3. P4, L12. The undercurrents are confined to west of 82.5E only for the month of March. During June, it extends till 83.5E. That should be roughly 180 km wide. I would say that the under currents are broader during summer compared to spring. Also, why is the width of undercurrents kept as 140 km in the abstract? The value is never mentioned in the text anywhere. Same goes for the maximum speed of 45 cm/s.

   (2) Width of the undercurrent varies seasonally, as does the depth and location of the velocity maximum core. Table 1 and 2 (above) have also been added to provide information about the characteristics of the undercurrent. The original text was not clear and we have revised the manuscript. The revised text and additional tables can be found in our response to Reviewer

Comment (2). In addition, we have removed the comment about the width of the undercurrent being 140 km in the abstract.

.

4. P4, L35. The strongest southward undercurrent during March-April is not very evident in the observations, especially in the glider data. For the CTD-Argo data, there is no evident undercurrent in April, when the strongest sub-surface flow is observed.

(2) The spring (March-April) undercurrent appears weaker in the observations (both CTD-Argo and glider data) compared to the OGCMs. Both depth and longitudinal position of the spring undercurrent core changes from year to year. This can mask the actual depth and longitude of the subsurface undercurrent in a sparsely sampled dataset such as the CTD-Argo profiles. We have made this point clearer in the revised manuscript. We have also included more recent Argo profiles into the calculation for Figure 3 and added arrows to each panel in the figure to make the presence of the undercurrent clearer to the reader.

(3) The manuscript has been revised (P4, L35-39).
"The spring undercurrent exists in all years in the model simulations except for in 2007 and 2011 in HYCOM when an El Niño occurs in the preceding year. POP also shows a weakening of the spring undercurrent following an El Niño event, except in 1998 when the northward-flowing surface current is absent and the southward current extends from the surface to approximately 550 m depth."

The manuscript has been revised (P5, L30-37).
"An undercurrent flowing in the opposing direction to the surface current is a prominent and consistent feature among the observations and OGCMs in boreal spring (beginning of February to mid-April) and summer (beginning of June to mid-August) (Figure 3). In boreal spring, the southward-flowing undercurrent extends from approximately 200 to 900 m depth with a velocity maximum core in the range of 300-600 m depth. The velocities derived from hydrography and Argo profiles and glider measurements confirm the existence of the undercurrent below 150-250 m, although the magnitudes are not consistent (Figure 3). This may be due to interannual variation in intensity and position of the subsurface reversed flow, combined with the sporadic sampling of the hydrography and Argo data."

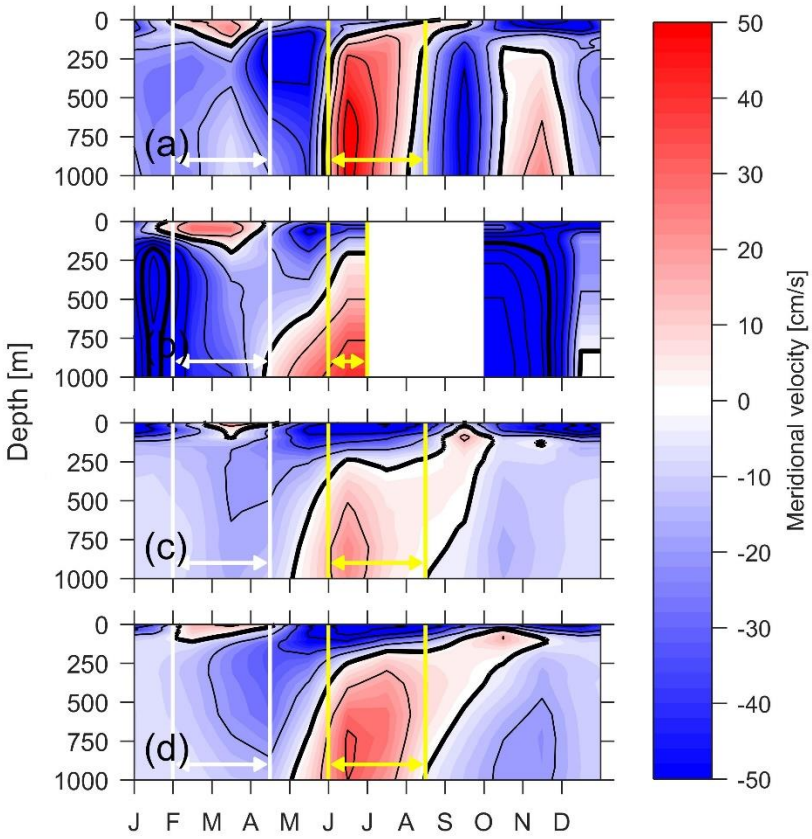

Figure 3. Bimonthly mean seasonal variation of the meridional geostrophic velocity referenced to the surface satellite ADT across the magenta transect in Figure 1 from hydrography and Argo measurements (a), glider measurements (b), monthly mean meridional velocity profiles from HYCOM (c), and POP (d) output. Line contours are plotted in the same manner as in Figure 2. White and yellow lines indicate periods when the undercurrent is most pronounced.

5. P4, L35. In the previous line, it is mentioned that the core of the undercurrent is observed at around 300 m. All of a sudden, without any justification, the undercurrents at 729 m is shown to highlight the spatial circulation. As the core of undercurrent changes from season to season, a decent justification should be provided to pick the 729 m depth. How different is the circulation at 729 m from that of 300 m?

   (2) The depth of the undercurrent core fluctuates from season to season and from year to year. In boreal spring (March-April), the depth of the undercurrent is shallower (300-600 m), while the summer (June-July) maximum velocity core is at ~900 m. The POP depth level at 729 m is selected as a representative depth of the undercurrent during both seasons. Nonetheless, we realize that the definition of the depth level should have occurred earlier in the manuscript. We have revised the manuscript to better justify the choice of this depth level for the undercurrent. The circulation patterns in the POP model along the eastern and southern coasts of Sri

Lanka are very similar at 318 m and 729 m, although the current is stronger at 318 m.

(3) *The manuscript has been revised (P6, L4-19).*
"To gain a better understanding of the subsurface circulation, we examine the POP velocity fields at 729 m (Movie S1), which encompasses the depth location of the undercurrent core in boreal spring and summer (Figures 2, 3; Tables 1, 2). In March, the undercurrent is strong and confined to 82.5° E along the entire Sri Lankan east coast (Movie S1). The undercurrent usually turns eastward around 6° N to combine with an eastward-flowing current along the Sri Lankan south coast, as shown in the simplified schematic derived from the POP 729 m velocity fields (Figure 4a). However, in some years (e.g. 1995, 1999, 2005, and 2007), the undercurrent turns westward around the southern coast of Sri Lanka and forms a narrow current, about 50-70 km wide, on the northern side of the eastward flow (Movie S1; Figure 4a). Note that a similar circulation is observed in the POP velocity fields at 318 m in March, albeit the flow is stronger. In boreal summer, there is a convergence of the eastward-flowing current along the south coast of Sri Lanka and a westward-flowing current in the southwestern BoB at approximately 7° N, 82.25° E (Movie S1), which is also shown in the simplified schematic (Figure 4b). Both OGCMs agree that the convergence produces the undercurrent flowing north along the east coast of Sri Lanka that injects relatively saline water into the BoB. In addition, an anticyclonic eddy often develops along the east coast, trapping local saline water inside, which is then propagated northward with the eddy (Movie S1)."

6. P5, L1-11. The evidence of upward phase propagation (generally implies remote forcing) is not highlighted here. The phase propagation is possibly caused by interior Ekman pumping (McCreary et al. 1996, Fig 6c), and is not observed during spring. Note that the propagation is not evident in the CTD/Argo data though.

(2) As the reviewer notes, upward phase propagation, especially during the summer, is evident in both OGCM outputs. We have now added text in the Discussion of the manuscript describing how this upward phase propagation relates to the passage of planetary waves. We thank the reviewer for pointing out this oversight.

(3) *The manuscript has been revised (P5, L41).*
"The OGCMs also suggest an upward phase propagation during summer and early fall (May- October) with a speed of approximately 1.5 m day^{-1} in the upper 200 m of the water column (Figure 3c, d). This feature is also evident in the geostrophic velocity derived from hydrography-Argo profiles in the upper 100 m of the water column (Figure 3a)."

Discussion of the upward phase propagation has also been added (P7, L24-27).
"Upward phase propagation is present during summer and early fall (Figure 3) implying the influence of equatorial waves on the subsurface flow during this time (Luyten and Roemmick, 1982). Equatorial waves are also known to

impact currents along the Indian east coast (Mukherjee et al., 2014) and Sri Lankan south coast (Schott et al., 1994; Shankar et al., 2002).”

7. P5, L19-22. Why is the statistics presented only for fall and winter? Please show for other seasons too and tabulate them.

(2) The statistics were only presented in winter in the original text to show that the winter subsurface flow is quite variable compared to its mean – this supports our suggestion that the winter undercurrent is not a permanent feature. However, we agree with the reviewer that the statistics should be presented for all seasons to highlight the existence of a spring and summer undercurrent and show that the fall and winter undercurrent are not permanent features. Hence, we have added Figure 5 (below) of the mean volume transport and the standard deviation computed from the OGCMs over the upper (0-200 m) and lower (200-1000 m) layer to show the size of the uncertainty of the undercurrent transport in each month compared to its mean. Volume transport computed from glider velocity referenced to its depth-averaged velocity in March and June when the undercurrent is distinct is also added to the figure for comparison.

(3) *A figure of volume transport in 0-200 m, 200-1000 m, and 0-1000 m layers has been added.*

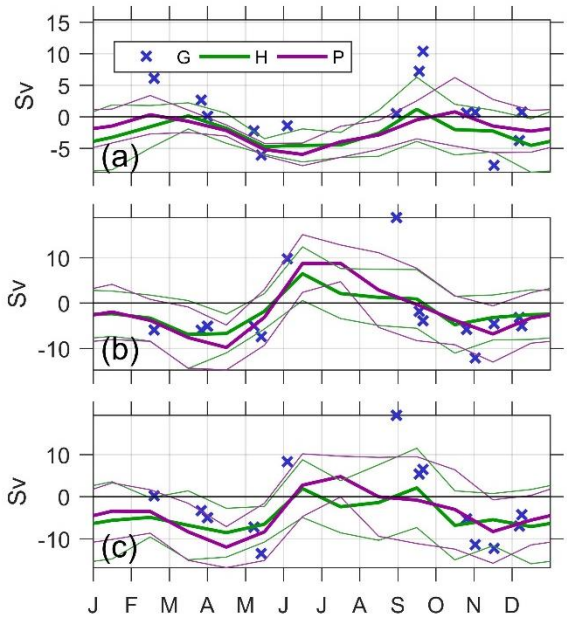

Figure 5. Meridional volume transport across 8° N from the Sri Lankan east coast to 82.5° E (dashed line in Figure 2) calculated from glider geostrophic velocity referenced to the depth-averaged velocity (G; blue cross) and absolute velocity fields from HYCOM (H; thick green line) and POP (P; thick purple line) over the 0-200 m (a), 200-1000 m (b), and 0-1000 m (c) layers. Thin lines designate the mean value +/- one standard deviation.

8. P6, L1. How does undercurrent play an important role in salt exchange, when it is mentioned later in the text that its contribution is only 1% of the total salt transport in BoB? This is even mentioned in the abstract. The statement should be made more clear.

(2) As the reviewer notes, the role of the undercurrent in the salt exchange between the basins is still unclear. We have moderated the influence of the salt exchange attributed to the undercurrent in the revised text (Discussion found in our response to Reviewer Comment (13) and Abstract) so as to better reflect the uncertainty of the salt exchange.

(3) The manuscript has been revised (P8, L24- P9, L12).

"Although velocity and salinity fields from POP suggest the possibility of significant salt exchange between the AS and the BoB, the estimated salt transport via the undercurrent is small based on the data and models we have available. POP velocity fields show that the summer undercurrent injects relatively saline water into the western boundary of the BoB that can be trapped in a northward-propagating seasonal anticyclonic eddy (Figure 4b). The source of the saline water is mostly from the southwest of Sri Lanka, although sometimes, such as in 1998, it originates from the eastern BoB (Movie S1). Relatively fresher water is transported southward along the east coast of Sri Lanka in the subsurface layer in spring (Figures 4a, 7). It can be advected westward along the Sri Lankan south coast in some years depending on the strength and location of the deep eastward-flowing Wyrtki jet (Reppin et al., 1999; Movie S1). The time series of salinity averaged over the width of the undercurrent (from the east coast of Sri Lanka to 82.5°E) and the volume transport of the POP undercurrent (over 200-1000 m) along 8°N clearly show a positive correlation i.e. the undercurrent tends to export freshwater from the BoB and import saline water into the BoB (Figure 7). The hydrography-Argo profiles, glider measurements, and HYCOM also show that poleward subsurface transport is associated with relatively saline water and vice versa (not shown). The correlation coefficient between the subsurface transport and salinity computed from POP is 0.50, significant at the 95% confidence level. The salt flux due to the fluctuations of the flow and of the salinity (departures from the 13-year climatology) in the 200-1000 m layer from POP is 0.04×10^6 kg s^{-1} (Figure 7), while the estimated salt flux from the hydrography-Argo profiles and glider measurements are 0.19×10^6 and 0.09×10^6 kg s^{-1}, respectively. The difference between the observational and POP salt fluxes arises from the smaller salinity range of the model compared to the observations (Table 3). The estimated salt input is up to 4% of the total expected salt transport into the BoB of 4.5-4.9$\times10^6$ kg s^{-1}, which is estimated from the annual freshwater input of 0.13-0.14 Sv (Rao and Sivakumar, 2003; Sengupta et al., 2006; Wilson and Riser, 2016). Note that the total net salt transported by POP into the BoB across 8°N is 4.3×10^6 kg s^{-1}; this value is in good agreement with the expected salt transport discussed above. Estimates of salt flux by the mean flow over the same depth layer from POP and HYCOM are even smaller: the mean undercurrent transport of 1.5-2 Sv in the OGCMs is fresher than the interior northward flow as judged from HYCOM and sparse hydrography and Argo profiles (not shown), but the salinity contrast at this depth layer is smaller than 0.01. In addition, the small salt

transport from the mean flow in the 200-1000 m layer might be due to the core of the undercurrent moving vertically such that this layer may sometimes include opposite flows or smaller salinity contrasts with the interior (Figures 2, 3; Table 1, 2).”

A table showing mean transport in boreal spring and summer and seasonal salinity range is added.

	Mean transport (Sv)		Seasonal salinity range
	Spring	Summer	
Hydrography -Argo	-6.9	9.7	0.09
Glider	-5.7	11.42	0.04
HYCOM	-4.6	3.0	0.01
POP	-5.7	6.8	0.01

Table 3. Mean transport and seasonal salinity range of the undercurrent (200-1000 m) across 8°N in boreal spring (February to mid-April as highlighted by white lines in Figure 3) and summer (June to mid-August as highlighted by yellow lines in Figure 3) from hydrography-Argo profiles, glider measurements, HYCOM, and POP. Seasonal salinity range is the approximate difference between boreal spring and summer extremes in average seasonal cycle. Note that the statistics representing glider measurements are derived from gridded velocity referenced to its depth-averaged velocity (e.g. Figure 2) and salinity interpolated onto 8°N.

The abstract has been revised.
“The existence of a seasonally varying undercurrent along 8° N off the east coast of Sri Lanka is inferred from shipboard hydrography, Argo floats, glider measurements, and two Ocean General Circulation Model simulations. Together, they reveal an undercurrent below 100-200 m flowing in the opposite direction to the surface current that is most pronounced during boreal spring and summer and switches direction between these two seasons. The volume transport of the undercurrent (200-1000 m layer) can be more than 10 Sv in either direction, exceeding the transport of 1-6 Sv carried by the surface current (0-200 m layer). The undercurrent transports relatively fresh water southward during spring, while it advects more saline water northward along the east coast of Sri Lanka during summer. Although the undercurrent is potentially a pathway of salt exchange between the Arabian Sea and the Bay of Bengal, the observations and the OGCMs suggest that the salinity contrast between seasons and between the boundary current and interior is less than 0.09 in the subsurface layer, suggesting a small salt transport by the undercurrent of less than 4% of the salinity deficit in the Bay of Bengal.”

9. P7 1-12. What is the surface current transport, undercurrent current transport, and the total transport at 8N? Please quantify them. Do undercurrents roughly follow the total transport or not? Try replicating Figure 4 of McCreary et al. (1996) at 8N. The ship drift velocity could be replaced with the undercurrent velocity or transport. I’m curious.

Because, the transport reverses during the summer monsoon along the east coast of India and not the surface circulation (McCreary, 1996). Therefore, the surface currents have a strong annual cycle, whereas the transport has a semiannual cycle. Is the reverse true here?

(2) As noted above, we have added Figure 5 to the revised manuscript to show the change in transport over different layers and the total 0-1000m layer. The OCGMs show that the surface transport (0-200 m) reverses twice a year. The undercurrent (200-1000 m) has strong northward flow during the summer (June-July) and southward flow during the spring (March-April), both in the opposite direction to the surface current. During the winter, volume transport over the 200-1000 m depth is still southward but weak. Transport over the depth range 0-1000 m in the water column is most closely related to the subsurface structure. Unfortunately, this figure is difficult to compare to the volume transport plotted in Figure 4 of McCreary et al. (1996) as the transport is given relative to 1000 m, whereas the volume transport calculated in this paper is absolute transport. (The ship drift current only reflects the near surface current, whereas the focus of our paper is on the subsurface undercurrent).

(3) *Discussion on surface current transport, undercurrent transport, and the total transport have been analyzed and added to the text (P6, L30- P7, L4).*
"Monthly volume transports computed from the OGCMs and volume transport computed from the discrete glider sections (referenced to depth-average velocity; e.g. Figure 2) across the 8° N transect between the eastern coast of Sri Lanka and 82.5° E (Figure 1a) over the upper (0-200 m) and lower (200-1000 m) layers are presented in Figure 5. The seasonal variation from HYCOM, POP, and glider measurements agree well, especially in the subsurface layer. Mean volume transport in the upper layer (0-200 m) has a semi-annual cycle that ranges from 1 to 6 Sv into and out of the BoB (Figure 5a). Southward flows are observed in the surface layer during boreal summer and winter. The flows are weakly northward during boreal spring and fall. Depth-integrated transport in the subsurface layer is southward throughout the year except during the summer when the northward-flowing undercurrent is present (Figures 3, 5b). The undercurrent transport is approximately 5-7 Sv out of and 3-11 Sv into the BoB during boreal spring and summer, respectively (Table 3). Moreover, the OGCMs suggest only a small mean volume transport of the subsurface current during fall and winter compared to its standard deviation (Figure 5b) implying that the fall and winter undercurrent is not well defined in these seasons and indeed can flow northward in some years. Volume transport over the 0-1000 m layer ranges from -12 to 5 Sv and exhibits an annual cycle similar to that in the lower (200-1000 m) layer (Figure 5c)."

More discussion is added to the discussion section of the manuscript (P7, L35-39).
"During the winter, the mean subsurface current of the observations and OGCMS agrees with the results from the LSM (McCreary et al., 1996) within

one standard deviation. This implies that a combination of local alongshore winds, Ekman pumping, and equatorial waves, which are the main mechanisms driving the subsurface current during the winter in the LSM, is important in producing the subsurface current in only some years."

10. P7 14-25. Why is the comparison made between Mindanao undercurrent (which in the Pacific Ocean)? Undercurrents are present all around the world. A general comparison would have made more sense. I would have preferred a comparison with the undercurrents observed along the east coast of India. The dynamics of both these regions are interlinked. For example, direct current measurements show that the seasonal undercurrents are not very prominent (in the top 300 m) north of 12N (See Mukherjee et al. 2014) along the east coast of India. The undercurrents at 12N are evident at a shallower depth and are present because of strong upward phase propagation. A similar comparison with earlier hydrographic observations could also be made where the transport estimates are available.

    (2) Our original thought was to compare and contrast the Sri Lanka undercurrent with other low latitude boundary currents, such as the Mindanao Current. However, we agree with the reviewer that a comparison with undercurrents observed in the BoB is more relevant. In the revised text the undercurrent off the Sri Lankan east coast is now discussed in the context of the undercurrents along the Indian east coast (the EICC- reported in Mukherjee et al., 2014) and the Sri Lankan south coast (SMC and WMC- reported in Schott et al., 1994). The comparison has been added to the discussion section found in our response to the Reviewer Comment (13).

    (3) The comparison has been added to the text (P8, L1-22).
    "Circulation in the subsurface layer along the Sri Lankan east coast is characterized by reversed flows relative to the surface during boreal spring and summer similar to the subsurface circulation along the Indian east coast and Sri Lankan south coast described by previous studies (Schott et al., 1994; McCreary et al., 1996; Mukherjee et al., 2014). During the southwest monsoon, the current along the Sri Lankan south coast (Schott et al., 1994), Sri Lankan east coast (Figure 2d-f; Table 2), and Indian east coast (Mukherjee et al., 2014) reverses its direction below approximately 100-150 m. The subsurface current flows eastward along the southern coast of Sri Lanka (Schott et al., 1994) in agreement with the circulation pattern derived from the POP velocity fields (Figure 4b) and poleward along the Sri Lankan and the Indian east coast (McCreary et al., 1996; Mukherjee et al., 2014). This suggests the possibility of a subsurface conduit connecting the region off the Sri Lankan south coast to the northern BoB. However, the subsurface poleward current along the Indian east coast is not always apparent (Mukherjee et al., 2014), although it is also possible that the undercurrent during this season occurs below the deepest measurement at 300 m from the Mukherjee et al. (2014) study. In boreal spring, mooring measurements along the Sri Lankan south coast (Schott et al., 1994) verifies the existence of the eastward-flowing subsurface current observed in the POP velocity fields (Figure 4a). The subsurface current extends from approximately 250 m to

1010 m (Schott et al., 1994). Unlike the summer subsurface circulation, flow at and north of 12° N is poleward over 0-300 m (Mukherjee et al., 2014), in the opposite direction to the undercurrent off the Sri Lankan east coast (Figures 2a-c, 3). However, since the core location of the spring undercurrent is highly variable from year to year, direct velocity measurements in the deeper layer would help to gain a better understanding of the pathways of the subsurface circulation along the western boundary of the BoB during boreal spring."

11. Theoretical studies have shown a presence of undercurrents during the winter (McCreary et al. 1996). This difference has not been highlighted well in the study. The absence of the winter undercurrent leads to an annual cycle, which is in contrast to surface currents, where the semi-annual component is prominent. Note that the winter undercurrent is present in the CTD-Argo data implying the presence of semi-annual cycle during some years. This point is not mentioned in the text.
    (2) The reviewer is correct, the difference between the mean undercurrent presented in the theoretical study (McCreary et al., 1996) and this study was not well highlighted. Our new Figure 5 presents the seasonal cycle of the mean transport in 0-200 m, 200-1000 m, and 0-1000 m. In the revised manuscript, we have discussed the difference between the findings of McCreary et al. (1996) and our study. Discussion of the seasonal cycle of the surface and subsurface current can be found in our response to Reviewer Comments (7) and (9).
12. It would be good to summarize the characteristics of undercurrents in a table. For example, you could divide the columns into seasons and mention the transport estimates, maximum current velocity, depth of the maximum velocity, and their necessary statistics (from both observations and model).
    (2) We thank the reviewer for the suggestion. We have added Tables 1 and 2 to summarize the characteristics of the undercurrent (see our response to Reviewer Comment (2)). Only the characteristics during March and June are summarized as the undercurrent is only prominent during these months and is not significant during fall and winter (Fig. 2 and 3 in the main text and Fig. 5).
13. The discussion section, in general, could be improved. The authors should further note that currents along the coast of Sri Lanka are complex. The complexity arises because the contribution from each of the forcing varies from year to year. For example, the climatology of alongshore currents from ship drift data show equatorward flow south of 8N (Mukherjee et al. 2014), and the satellite data shows an annual cycle both south and north of 8N (Mukherjee et al 2014, Lee et al 2016). It's around 8N that the semi-annual cycle is more evident and this location may not represent the actual circulation along the entire Sri Lankan east coast.
    (2) The reviewer is correct, the circulation across 8° N has a very complex structure as it represents interactions between different currents, such as the SMC/ WMC and the EICC, as well as the effect of strong wind stress curl and equatorial waves. All these phenomena vary on interannual time scales. We have revised our Discussion section to better recognize this complexity as suggested by the reviewer. In addition, we note that our new Figure 5a shows

the semi-annual signal in the surface layer that agrees with the ship drift data as pointed out by the reviewer. Nonetheless, the focus of our study is on the subsurface undercurrent and trying to better understand its characteristics.

(3) *The discussion section has been revised (P7, L5- P9, L24).*

"The circulation in the southern BoB is complex as it is controlled by various forcings, such as local winds, Ekman pumping, and equatorial waves, which impact the region in different seasons. The mechanisms driving the undercurrent remain unclear and although beyond the scope of this study we put forward some informed hypotheses based on previous studies and our observations. The Rossby waves, equatorial waves, and Ekman pumping are likely to be important for producing the undercurrent: a Hovmöller diagram of POP meridional velocity across 8° N (Figure 6) shows the westward propagation of the velocity signal at 729 m depth originating from the eastern boundary of the BoB that takes about four months to cross the southern BoB. It has a propagation speed of 12 cm s^{-1} in good agreement with the phase speed of a mode 2 baroclinic Rossby wave in this region (Shankar et al., 1996; Killworth and Blundell, 2003; Wijesekera et al., 2016a). A westward-propagating signal first develops at the eastern boundary of the BoB in April-May at the same time that the Wyrtki Jet, a surface-intensified eastward-flowing current observed in the equatorial Indian Ocean during the monsoon transitions (Wyrtki, 1973), reaches this eastern boundary. The westward-propagating signal reaches the east coast of Sri Lanka in September contributing to the southward-flowing subsurface current (Figures 3); this is consistent with findings from the LSM study (McCreary et al., 1996). In April, the westward propagating meridional flows originating at 83° E-85° E (Figure 6b) are associated with the subsurface anticyclonic eddy observed along the east coast of Sri Lanka during the summer (Figure 4b). The influence of equatorial waves on the undercurrent is still unclear and more studies are needed. Upward phase propagation is present during summer and early fall (Figure 3) implying the influence of equatorial waves on the subsurface flow during this time (Luyten and Roemmick, 1982). Equatorial waves are also known to impact currents along the Indian east coast (Mukherjee et al., 2014) and Sri Lankan south coast (Schott et al., 1994; Shankar et al., 2002).

Ekman pumping can also significantly impact the circulation along the eastern coast of Sri Lanka (McCreary et al., 1996; Vinayachandran et al., 1999). The LSM study of McCreary et al. (1996) suggested that Ekman pumping drives the undercurrent east of Sri Lanka from April to December. The model undercurrent has a core at 400-500 m that can reach a maximum speed of 10 cm s^{-1} southward and northward in March-April and August, respectively. Although this value agrees quite well with that of the spring undercurrent observed in the observations and OGCMs, the magnitude given by the LSM during the summer is about half that shown in this study (Figure 3). During the winter, the mean subsurface current of the observations and OGCMS agrees with the results from the LSM (McCreary et al., 1996) within one standard deviation. This implies that a combination of local alongshore winds,

Ekman pumping, and equatorial waves, which are the main mechanisms driving the subsurface current during the winter in the LSM, is important in producing the subsurface current in only some years.

Circulation in the subsurface layer along the Sri Lankan east coast is characterized by reversed flows relative to the surface during boreal spring and summer similar to the subsurface circulation along the Indian east coast and Sri Lankan south coast described by previous studies (Schott et al., 1994; McCreary et al., 1996; Mukherjee et al., 2014). During the southwest monsoon, the current along the Sri Lankan south coast (Schott et al., 1994), Sri Lankan east coast (Figure 2d-f; Table 2), and Indian east coast (Mukherjee et al., 2014) reverses its direction below approximately 100-150 m. The subsurface current flows eastward along the southern coast of Sri Lanka (Schott et al., 1994) in agreement with the circulation pattern derived from the POP velocity fields (Figure 4b) and poleward along the Sri Lankan and the Indian east coast (McCreary et al., 1996; Mukherjee et al., 2014). This suggests the possibility of a subsurface conduit connecting the region off the Sri Lankan south coast to the northern BoB. However, the subsurface poleward current along the Indian east coast is not always apparent (Mukherjee et al., 2014), although it is also possible that the undercurrent during this season occurs below the deepest measurement at 300 m from the Mukherjee et al. (2014) study. In boreal spring, mooring measurements along the Sri Lankan south coast (Schott et al., 1994) verifies the existence of the eastward-flowing subsurface current observed in the POP velocity fields (Figure 4a). The subsurface current extends from approximately 250 m to 1010 m (Schott et al., 1994). Unlike the summer subsurface circulation, flow at and north of 12° N is poleward over 0-300 m (Mukherjee et al., 2014), in the opposite direction to the undercurrent off the Sri Lankan east coast (Figures 2a-c, 3). However, since the core location of the spring undercurrent is highly variable from year to year, direct velocity measurements in the deeper layer would help to gain a better understanding of the pathways of the subsurface circulation along the western boundary of the BoB during boreal spring.

Although velocity and salinity fields from POP suggest the possibility of significant salt exchange between the AS and the BoB, the estimated salt transport via the undercurrent is small based on the data and models we have available. POP velocity fields show that the summer undercurrent injects relatively saline water into the western boundary of the BoB that can be trapped in a northward-propagating seasonal anticyclonic eddy (Figure 4b). The source of the saline water is mostly from the southwest of Sri Lanka, although sometimes, such as in 1998, it originates from the eastern BoB (Movie S1). Relatively fresher water is transported southward along the east coast of Sri Lanka in the subsurface layer in spring (Figures 4a, 7). It can be advected westward along the Sri Lankan south coast in some years

depending on the strength and location of the deep eastward-flowing Wyrtki jet (Reppin et al., 1999; Movie S1). The time series of salinity averaged over the width of the undercurrent (from the east coast of Sri Lanka to 82.5°E) and the volume transport of the POP undercurrent (over 200-1000 m) along 8°N clearly show a positive correlation i.e. the undercurrent tends to export freshwater from the BoB and import saline water into the BoB (Figure 7). The hydrography-Argo profiles, glider measurements, and HYCOM also show that poleward subsurface transport is associated with relatively saline water and vice versa (not shown). The correlation coefficient between the subsurface transport and salinity computed from POP is 0.50, significant at the 95% confidence level. The salt flux due to the fluctuations of the flow and of the salinity (departures from the 13-year climatology) in the 200-1000 m layer from POP is 0.04×10^6 kg s^{-1} (Figure 7), while the estimated salt flux from the hydrography-Argo profiles and glider measurements are 0.19×10^6 and 0.09×10^6 kg s^{-1}, respectively. The difference between the observational and POP salt fluxes arises from the smaller salinity range of the model compared to the observations (Table 3). The estimated salt input is up to 4% of the total expected salt transport into the BoB of $4.5\text{-}4.9\times10^6$ kg s^{-1}, which is estimated from the annual freshwater input of 0.13-0.14 Sv (Rao and Sivakumar, 2003; Sengupta et al., 2006; Wilson and Riser, 2016). Note that the total net salt transported by POP into the BoB across 8°N is 4.3×10^6 kg s^{-1}; this value is in good agreement with the expected salt transport discussed above. Estimates of salt flux by the mean flow over the same depth layer from POP and HYCOM are even smaller: the mean undercurrent transport of 1.5-2 Sv in the OGCMs is fresher than the interior northward flow as judged from HYCOM and sparse hydrography and Argo profiles (not shown), but the salinity contrast at this depth layer is smaller than 0.01. In addition, the small salt transport from the mean flow in the 200-1000 m layer might be due to the core of the undercurrent moving vertically such that this layer may sometimes include opposite flows or smaller salinity contrasts with the interior (Figures 2, 3; Table 1, 2).

An alternative interbasin-exchange pathway is through the interior of the BoB, particularly during the southwest and northeast monsoon (Vinayachandran et al., 1999; Wijesekera et al., 2015; Wijesekera et al., 2016b). Observations indicate that the eastward-flowing southwest monsoon current (SMC) has a role in the injection of saline water originating in the AS into the southern central BoB during early summer. As the summer progresses, the seasonal cyclonic (i.e. the SLD) and anticyclonic eddies influence the pathway of the SMC (Vinayachandran and Yamagata, 1997; Vinayachandran et al., 1999). Mooring observations at 85.5°E from 5°N to 8°N reveal a northward-flowing subsurface SMC that is associated with high salinity water (Wijesekera et al., 2016a; Wijesekera et al., 2016b). During the northwest monsoon, mass and salt exchange between the AS and the BoB is also observed in the interior

over the 50-75 m layer in the southern BoB, approximately between 82.5°E and 85 °E (Wijesekera et al., 2015).”

Anonymous Referee #2 Received and published: 23 August 2017

1. The literature review of the authors is inadequate. Many of the papers which talk about under currents around Sri Lanka are not mentioned. For example, Schott et al., JGR, 1994 which talks about opposite directions of surface and sub-surface currents. K1 mooring at 5.5N shows opposite currents during July-Aug. Wijesekera et al., JPO 2016 uses ADCP data to describe the surface and subsurface currents at 5-8^{o} N off east coast of Sri Lanka. Shankar et al., 2002 PIO is not mentioned, which talks about currents at 8N.

   (2) We thank the Reviewer for this suggestion and for the references. Our literature review has now been revised. We include a discussion on the undercurrent along the Indian east coast (EICC) and the Sri Lanka south coast (SMC/ WMC).

   (3) The literature review has been revised (P1, L32 – P2, L31).
   “The surface current to the east of Sri Lanka is influenced by local alongshore winds, remote winds in the vicinity of the northern and eastern boundaries of the BoB, equatorial waves, and interior Ekman pumping (Yu et al., 1991; Shetye et al., 1993; McCreary et al., 1996; Shankar et al., 1996; Vinayachandran and Yamagata, 1997). This current has a strong seasonal pattern (Shankar et al., 2002; Lee et al., 2016) with recirculation loops that are highly variable in time and space (Durand et al., 2009). Some of the recirculations appear seasonally, such as the Sri Lanka Dome (SLD), a cyclonic eddy that is well developed in July (Vinayachandran and Yamagata, 1997). The SLD is driven by Rossby waves radiating from the eastern boundary and intensified Ekman pumping inside the BoB (Vinayachandran et al., 1999; Shankar et al., 2002; de Vos et al., 2014). The SLD propagates westward (Wijesekera et al., 2016b) toward the east coast of Sri Lanka resulting in a southward coastal surface flow during early summer. In October, the prevailing wind in the BoB starts reversing direction and blows southwestward. This marks the start of the northeast monsoon when the local wind along the east coast of India drives the East India Coastal Current (EICC) southward with speeds exceeding 1 m s^{-1} extending from the east coast of India southward to the southern tip of Sri Lanka (Shetye et al., 1996; Wijesekera et al., 2015).

   The subsurface circulation in this region is also potentially important as high-salinity water from the AS can be subducted beneath the fresher surface water originating from river runoff and precipitation in the northern BoB (Rao & Sivakumar, 2003; Sengupta et al., 2006; Vinayachandran et al., 2013; Gordon et al., 2016; Jensen et al., 2016); this is evident in observations and model studies both during the northeast (Wijesekera et al., 2015) and southwest monsoons (June- August) (Wijesekera et al., 2016b). Little is known about the subsurface structure of the boundary current along the east coast of Sri Lanka. Mooring observations show a reversing subsurface current occurring off the southern coast of Sri Lanka; it is most distinct during

boreal spring and summer (Schott et al., 1994). In addition, reversal of the EICC along the east coast of India is observed below 100 m that is southward during the southwest monsoon and northward during the northeast monsoon, with the winter undercurrent being a more permanent feature (Mukherjee et al., 2014). The direction of this undercurrent is in good agreement with findings from a linear, continuously stratified ocean model (LSM) (McCreary et al., 1996). The LSM also suggests the presence of an undercurrent along the Sri Lankan east coast (centered at 8^{o} N) that reverses its direction twice a year with model speeds ranging from 6 cm s^{-1} equatorward during boreal spring to 8 cm s^{-1} poleward during summer. This undercurrent has not been observed before and will be the focus of this study. We will investigate the vertical structure and seasonal variability of subsurface flows in the boundary current system off the eastern coast of Sri Lanka using OGCMs as well as observations from shipboard hydrography, Argo floats, and glider measurements. Knowledge of the vertical structure, variability, and associated dynamics of the boundary current will contribute to a better understanding of mass and salt exchanges in the northern Indian Ocean."

2. Page No. 4 lines 23-25: The surface current reverses its direction four times a year ….
   Comment: I do not think it is a correct statement. Shetye et al., 1996 talks about EICC during northeast monsoon. McCreary et al., 1996 talks about two times change in EICC direction, Durand et al., 2009 does not mention about four times change in the current direction. It would be better if authors can draw a schematic diagram to represent the EICC directions as studied by the afore mentioned papers and compare it with present study.
   (2) The reviewer is correct and we have revised the statement
   (3) The statement is corrected (P5, L13-14).
   "The surface current reverses its direction twice a year."

3. Page No. 6 lines 22, 27: A westward -propagating southward current....
   The westward propagating northward and southward flows...
   Comment: What do authors means by that? It is totally confusing. A similar Hovmoller diagram is shown in Shankar et al., 2002. Authors can read that and describe this figure in a better way.
   (2) The statements describing the figure have now been revised to avoid confusion.
   (3) *The statement is revised (P7, L20-23).*
   "In April, the westward propagating meridional flows originating at 83° E-85° E (Figure 6b) are associated with the subsurface anticyclonic eddy observed along the east coast of Sri Lanka during the summer (Figure 4b)."

4. Page 6 Lines 6-8: The undercurrent potentially plays an important role in salt and mass exchange between the AS and the BoB.
   Comment: But the movie shows that the dominant source of saline water is from eastern BoB. Very little contribution is from AS
   (2) The reviewer is correct that water from the AS is not the sole source and the eastern BoB is also likely to contribute saline water. However, the model shows that at 729 m depth, the majority of saline water from the eastern BoB

is transported westward along the Sri Lankan south coast. Only in a few years (for example 1998) is a coherent pattern not found between salinity along the southwestern and eastern coasts of Sri Lanka. The source of saline water advected by the undercurrent has been revised in the manuscript.

(3) *Clarification is added to the manuscript (P8, L26-29).*
"POP velocity fields show that the summer undercurrent injects relatively saline water into the western boundary of the BoB that can be trapped in a northward-propagating seasonal anticyclonic eddy (Figure 4b). The source of the saline water is mostly from the southwest of Sri Lanka, although sometimes, such as in 1998, it originates from the eastern BoB (Movie S1)."

5. Page 6 Lines 30-35: The stratified linear model study (McCreary et al., 1996) also indicates the role of ekman pumping ….
Comment: In McCreary et al., 1996 paper, at 8N, Equatorial forcing and Ekman pumping both look important for currents below 200m, though the current magnitude is very weak in both cases. The authors only say that ekman pumping is important without a convincing argument.

(2) We agree with the Reviewer, however there are presently no observations available that might support the argument, and so determining the mechanisms driving the undercurrent is beyond the scope of this study.

(3) *The discussion on possible driving mechanisms has been revised to clarify the point (P7, L7-10).*
"The circulation in the southern BoB is complex as it is controlled by various forcings, such as local winds, Ekman pumping, and equatorial waves, which impact the region in different seasons. The mechanisms driving the undercurrent remain unclear and although beyond the scope of this study we put forward some informed hypotheses based on previous studies and our observations. The Rossby waves, equatorial waves, and Ekman pumping are likely to be important for producing the undercurrent."

6. Page 6 Lines 30-35: The last paragraph of the discussion section, deals with currents in Pacific Ocean.
Comment: This seems completely out of context.

(2) This was also pointed out by Reviewer (1) in Reviewer Comment (10). Our original thought was to compare and contrast the Sri Lanka undercurrent with other low latitude boundary currents, such as the Mindanao Current. However, we agree with the reviewer that a comparison with undercurrents observed in the BoB is more relevant. In the revised text the undercurrent off the Sri Lankan east coast is now discussed in the context of the undercurrents along the Indian east coast (the EICC- reported in Mukherjee et al., 2014) and the Sri Lankan south coast (SMC and WMC- reported in Schott et al., 1994).

An Undercurrent off the East Coast of Sri Lanka

Arachaporn Anutaliya[1], Uwe Send[1], Julie L~~,~~. McClean[1], Janet Sprintall[1], Luc Rainville[2], Craig Lee[2], S. U. Priyantha Jinadasa[3], Alan J. Wallcraft[4], E. Joseph Metzger[4]

[1]Scripps Institution of Oceanography, La Jolla, California, USA
[2]Applied Physics Laboratory, University of Washington, Seattle, Washington, USA
[3]National Aquatic Resources Research and Development Agency, Colombo, Sri Lanka
[4]Naval Research Laboratory, Stennis Space Center, Mississippi, USA

Correspondence to: Arachaporn Anutaliya (aanutali@ucsd.edu)

Abstract. The existence of a seasonally varying undercurrent along 8° N off the east coast of Sri Lanka is inferred from ~~Conductivity-Temperature-Depth profiles~~shipboard hydrography, Argo floats, glider measurements, and two Ocean General Circulation Model ~~outputs~~simulations. Together, they reveal an undercurrent below 100-200 m ~~that is approximately 140 km wide and can reach a maximum speed of 45 cm s^{-1} that hitherto has not been observed. The undercurrent,~~ flowing in the opposite direction to the surface current~~,~~ that is most pronounced during boreal spring and summer and switches direction between these two seasons. The volume transport of the undercurrent (200-1000 m layer) can be more than 10 Sv in either direction, exceeding the transport of 1-6 Sv carried by the surface current (0-200 m layer). The undercurrent transports relatively fresh water southward during spring, while it advects more saline water northward along the east coast of Sri Lanka during summer. ~~This suggests a pathway, independent of the surface circulation, whereby freshwater is removed and saline water is injected into~~Although the undercurrent is potentially a pathway of salt exchange between the Arabian Sea and the Bay of Bengal, the observations and the OGCMs suggest that the salinity contrast between seasons and between the boundary current and interior is less than 0.09 in the subsurface layer, suggesting a small salt transport by the undercurrent of less than 4% of the salinity deficit in the Bay of Bengal.

1 Introduction

Knowledge of the circulation in the southern Bay of Bengal (BoB) is crucial to understanding the contrasting salinity distributions of the Arabian Sea (AS) and the BoB since it ~~determines~~controls the amount of water and salt exchanged between the two ocean basins. Observations and ~~model~~modeling studies have confirmed the role of the surface current along the Sri Lankan east coast in distributing mass and salt between the AS and the BoB. Drifters indicate that a strong surface-intensified current to the east of Sri Lanka during the northeast monsoon (~~boreal winter~~November- January) transports low-salinity water out of the BoB toward the AS around the south coast of Sri Lanka (Wijesekera et al., 2015). ~~A numerical~~An ocean general circulation model (OGCM) study also shows that significant mass and salt transport ~~occurs~~occur between the AS and the BoB along the ~~east~~eastern and ~~south~~southern coast of Sri Lanka (Jensen et al., 2016).

The surface current to the east of Sri Lanka is influenced by local alongshore winds, remote winds in the vicinity of the northern and eastern boundaries of the BoB, equatorial waves, and interior Ekman pumping (Yu et al., 1991; Shetye et al., 1993; McCreary et al., 1996; Shankar et al., 1996; Vinayachandran et al., and Yamagata, 1997). This current has a strong seasonal pattern (Shankar et al., 2002; Lee et al., 2016) with recirculation loops that are highly variable in time and space (Durand et al., 2009). Some of the recirculations appear seasonally, such as the Sri Lanka Dome (SLD), a cyclonic eddy that is well developed in July (Vinayachandran et al., and Yamagata, 1997). The SLD is driven by Rossby waves radiating from the eastern boundary and intensified Ekman pumping inside the BoB (Vinayachandran et al., 1999; Shankar et al., 2002; de Vos et al., 2014). The SLD propagates westward (Wijesekera et al., 2016b) toward the east coast of Sri Lanka resulting in a southward coastal surface flow during early summer. In October, the prevailing wind in the BoB starts reversing direction and blows southwestward. This marks the start of the northeast monsoon when the local wind along the east coast of India drives the East India Coastal Current (EICC) southward with speeds exceeding 1 m s^{-1} extending from the east coast of India southward to the southern tip of Sri Lanka (Shetye et al., 1996; Wijesekera et al., 2015).

The *subsurface* circulation in this region is also potentially important as high-salinity water from the AS can be subducted beneath the fresher surface water originating from river runoff and precipitation in the northern BoB (Rao & Sivakumar, 2003; Sengupta et al., 2006; Vinayachandran et al., 2013; Gordon et al., 2016; Jensen et al., 2016); this is evident in observations and model studies both during the northeast (Wijesekera et al., 2015) and southwest monsoons (June- August) (Wijesekera et al., 2016b). Little is known about the subsurface structure of the boundary current along the east coast of Sri Lanka. Mooring observations show a reversing subsurface current occurring off the southern coast of Sri Lanka; it is most distinct during boreal spring and summer (Schott et al., 1994). In addition, reversal of the EICC along the east coast of India is observed below 100 m that is southward during the southwest monsoon and northward during the northeast monsoon, with the winter undercurrent being a more permanent feature (Mukherjee et al., 2014). The direction of this undercurrent is in good agreement with findings from a linear, continuously stratified ocean model (LSM) (McCreary et al., 1996). The LSM also suggests the presence of an undercurrent along the Sri Lankan east coast (centered at 8 ^{o} N) that reverses its direction twice a year with model speeds ranging from 6 cm s^{-1} equatorward during boreal spring to 8 cm s^{-1} poleward during summer. This undercurrent has not been observed before and will be the

~~The purpose~~focus of this study ~~is to~~. We will investigate the vertical structure and seasonal variability of subsurface flows in the boundary current system ~~to~~off the ~~east~~eastern coast of Sri Lanka using ~~Ocean General Circulation Models (~~OGCMs~~)~~ as well as observations from ~~Conductivity-Temperature-Depth (CTD),~~shipboard hydrography, Argo floats, and glider measurements. Knowledge of the vertical structure, variability, and associated dynamics of the boundary current will ~~provide~~contribute to a better understanding of ~~salt~~mass and ~~mass~~salt exchanges in the northern Indian Ocean.

2 Data and Methodology

~~CTD~~Shipboard hydrography and Argo Conductivity-Temperature-Depth (CTD) profiles, together with satellite altimeter-derived surface absolute dynamic topography (ADT), were used to determine the vertical structure of the current east of Sri Lanka. There were ~~54 CTD~~13 shipboard hydrography and ~~20~~116 Argo profiles available between 7-9° N and within 130 km of the Sri Lankan east coast that sampled to at least 1000 m depth (Figure 1a). The ~~CTD~~hydrographic profiles were ~~sampled~~collected over the period of ~~1961- 2011~~2008-2017 while the Argo profiles were collected over ~~2005-2016~~2007-2017. The gridded delayed-time ADT products were derived from Archiving, Validation, and Interpretation of Satellite Oceanographic (AVISO) Data (Ducet et al., 2000) which are available over the period of 1993-2016 with spatial and temporal resolutions of ¼° latitude × ¼° longitude and 7 days, respectively.

The hydrography-Argo based mean seasonal absolute geostrophic meridional velocity profiles were calculated by combining sheared velocity profiles from ~~CTD~~hydrography and Argo measurements and surface velocity from the ADT products. ~~To~~The number of hydrography and Argo profiles available were too few to calculate robust estimates of monthly meridional geostrophic velocity. Hence, to derive the seasonal sheared velocity profiles, we used 2-month (*i.e.* bimonthly) sliding mean dynamic heights ~~from CTD profiles were~~ calculated ~~positioned~~ from hydrography-Argo profiles located to the west and east~~, within 50 km from the coast, and west, between 50-130 km from the coast, of the expected~~ of the central position of the boundary current~~. The number of CTD and Argo profiles available in each bimonthly period varied from 3 to 6 in the western region and from 3 to 16 in the eastern region (Figure 1b). The bimonthly mean~~ (Figure 1a); the position of the boundary current was determined from a longitude-depth velocity transect along 8° N derived from glider measurements and OGCMs (for example, Figure 2). The low-pass filtered geostrophic meridional sheared velocity profile is thus proportional to the corresponding difference between the eastern and western ~~mean bimonthly~~filtered dynamic heights. ~~Adding the bimonthly mean~~The number of hydrography and Argo profiles available in each bimonth period varied from 3 to 14 in the western region and from 4 to 24 in the eastern region (Figure 1b). The equally low-passed surface meridional velocity from the satellite ADT along 8° N between 81.75° E-82.5° E was added to the sheared profiles ~~yielded bimonthly~~to yield absolute geostrophic meridional velocity profiles.

Gliders were deployed to the east of Sri Lanka between 7° N and 9° N to collect salinity and temperature ~~measurements~~profiles from the surface to 1000 m depth ~~since February 2014 (Lee et al.,~~

~~2016) (Figure 1a). Temperature and salinity profiles collected from gliders~~ during February 2014–January 2016 (Lee et al., 2016) (Figure 1a). The geostrophic velocities from the glider measurements are referenced in two ways. Glider temperature and salinity profiles are used to calculate geostrophic velocity across 8° N referenced to the glider depth-averaged velocity to examine the vertical structure of the undercurrent (e.g. Figure 2). Note that profiles sampled by the gliders were sporadic in time; the gliders took approximately 2-7 days to complete the transect and then could take 5-30 days until the same transect was repeated. Thus, the glider velocity referenced to the depth-averaged current is less suitable to estimate the seasonal evolution of the circulation along Sri Lankan east coast (*i.e.* Figure 3). Instead, temperature and salinity profiles were used in the same way as the ~~CTD~~hydrography and Argo profiles to calculate bimonthly ~~sliding mean~~ geostrophic meridional ~~velocity. Absolute geostrophic velocity is obtained by referencing the profile to the depth-averaged~~ velocity.

Two global strongly eddy active OGCMs were used to study the vertical structure and seasonal variation of the boundary current ~~and the~~, as well as its associated dynamics: 0.1° ~~global~~ Parallel Ocean Program (POP) and 0.08° ~~global~~ HYbrid Coordinate Ocean Model (HYCOM). Their horizontal resolutions correspond to 11 km and 9 km at 8° N, respectively. POP is a three-dimensional, *z*-level, primitive equation model (Smith et al., 2010). It was configured on a global tripole grid with 42 vertical levels~~. Vertical~~ and partial bottom cells. Its vertical grid spacing near the surface (top 50m) is roughly 10 m. The POP simulation ~~analyzed in this study~~ was initialized from ~~Year~~year 30 of an earlier POP ~~simulation~~ run ~~on this~~that used the same ~~grid and~~set-up but was driven by a monthly climatology of Co-ordinated Ocean Reference Experiments (CORE) atmospheric surface fluxes (Maltrud et al., 2010). ~~Our analysis run~~The subsequent POP simulation was forced by interannually-varying CORE-II fluxes for 1990-2007 (Delman et al., 2015). The POP output analyzed here ~~are~~consists of three-dimensional daily-averaged velocities and salinity for 1995-2007. HYCOM has a hybrid vertical coordinate with isopycnal coordinates in the open stratified ocean, a terrain-following coordinate for coastal regions, and a *z*-level coordinate in the mixed layer (Metzger et al., 2010). It was configured on a global tripole grid with 41 vertical layers. Vertical grid spacing ~~near~~very close to the surface is roughly 1 m~~.~~ increasing to 8 m over 36-85 m. The simulation was forced by 3~~-~~-hourly Navy Operational Global ~~Forecasting~~Atmospheric Prediction System (NOGAPS) ~~atmospheric forcing~~fields (Rosmond et al., 2002). However, the archived velocity fields used here are monthly and cover a shorter period compared to POP of 2003-2012.

3 The Circulation east of Sri Lanka

~~An undercurrent~~ 3.1 Vertical structure

A zonal transect along 8° N is ~~defined here as~~ used to examine the ~~maximum velocity core of the subsurface flow that is separated from the~~circulation off the eastern coast of Sri Lanka. Both observations and OGCMs show a seasonally reversing surface current ~~by weak flow. Unambiguous cases exist when~~confined to the upper 100-200 m of the water column (Figures 2, 3). A subsurface ~~flow is~~current that flows in the opposite direction to that of the surface ~~flow. This~~water, defined here as an

undercurrent, is ~~clearly~~ observed from glider measurements and the OGCMs particularly in ~~longitude-depth transects of absolute~~March and June (Figure 2). As noted above, geostrophic ~~meridional~~ velocities ~~across 8° N~~ derived from glider measurements ~~and meridional velocities from the OGCMs (Figure 2). Glider geostrophic velocities were from measurements~~, during March 18-30, 2014 (Figure 2a) and May 28–June 8, 2014 (Figure 2d~~) and velocity~~), are referenced to the depth-averaged velocity measured directly by the gliders. Velocity transects from HYCOM (Figure 2b, e) and POP (Figure 2c, f) ~~are the~~ were constructed from monthly averages of total velocity in March and June for the periods of 2003-2012 and 1995-2007, respectively.

The model transects show ~~good~~reasonable agreement with that from the gliders in regard to the vertical structure~~, width, and intensity~~ of both the surface current and undercurrent. ~~The glider velocity transect in March 2014 shows the expected~~In March, the core of the observed undercurrent is located about 55 km from the coast and has a maximum speed of 16-25 cm s^{-1} southward (Table 1). HYCOM and POP have maximum flows in the reverse direction to the surface *i.e.* southward, at 570 and 268 m, respectively (Figure 2a-b) while glider measurements show maximum subsurface flow at the deepest measured depth of 1000 m (Figure 2c). In June, a northward undercurrent is observed below approximately 250 m with a maximum speed greater than 20 cm s^{-1} at about 900 m (Figure 2d-f; Table 2). The summer undercurrent is approximately 165 km wide in the OGCMs. The velocity section derived from gliders shows a wider undercurrent of 210 km with two cores: a deep core that is approximately 100 km wide centered at 82.2° E and a shallow core at 400 m near 82.75° E (Figure 2d). This double-core feature is also evident in some individual model years, but is not present in the multi-year mean (Figure 2e, f).

Investigation of individual years of HYCOM and POP velocity fields reveals that although the location of the undercurrent core varies in depth and longitude, it is nearly always confined to the west of 82.5° E. Thus, this longitude limit will be used in subsequent averages over the undercurrent regime, and is indicated by the dashed line in Figure 2. The spring undercurrent exists in all years in the model simulations except for in 2007 and 2011 in HYCOM when an El Niño occurs in the preceding year. POP also shows a weakening of the spring undercurrent following an El Niño event, except in 1998 when the northward-flowing surface current ~~along the east coast of Sri Lanka which is confined to the top 200 m of the water column (Figure 2a). This boundary current reverses its direction below 200 m with a subsurface velocity maximum core found below 800 m and a maximum speed greater than 25 cm s^{-1}. Both velocity transects from the OGCMs show similar results to the observations, except that the model mean surface~~is absent and the southward current extends ~~to approximately 100 m and the subsurface velocity maximum core is located between 400-600 m (Figure 2b,c). In June, both glider and OGCM results show the expected strong southward~~ from the surface ~~current in the 0-200 m layer (Figure 2d-f). A northward undercurrent is apparent at this time below 200 m with its maximum speed greater than 20 cm s^{-1} at about 800 m. During March and June, the undercurrent is confined to the west of 82.5° E and is approximately 85 km wide~~to approximately 550 m depth.

3.2 Seasonal variation

Bimonthly mean meridional velocities~~,~~ computed from ~~CTD~~hydrography and Argo profiles and glider measurements~~,~~ are shown in ~~Fig.~~Figure 3a and ~~b~~3b respectively. ~~Monthly~~These observed geostrophic velocities are all referenced to surface velocity from the ADT. The model monthly mean total meridional velocities (Figure 3c, d) were constructed from the OGCMs by averaging the monthly mean velocity across 8° N ~~over~~along the ~~width~~transect from the eastern coast of ~~the undercurrent between 81.75° E and~~Sri Lanka to 82.5° E (depicted by the magenta transect in ~~Fig. 1) (Figure 3c,d).~~ Figure 1), which captures most of the undercurrent signal (Figure 2; Table 1, 2).

3.2.1 Surface circulation

Both surface and subsurface currents have strong seasonal variability (Figure 3). The surface current reverses its direction ~~four times~~twice a year in agreement with previous studies (Yu et al., 1991; McCreary et al., 1996; Shetye et al., 1996; Vinayachandran and Yamagata, 1997; Vinayachandran et al., 1999; Eigenheer and Quadfasel, 2000; Durand et al., 2009; de Vos et al., 2014; Wijesekera et al., 2015; Lee et al., 2016). The mean meridional surface current is northward during boreal spring (Figure 2a-c, Figure 3) as the westward flowing North Equatorial Current often bifurcates at the east coast of Sri Lanka at approximately 7.5° N splitting into a northward and southwestward branch (Shetye et al., 1993; Hacker et al., ~~et al., 1997; Vinayachandran et al., 1999; Durand et al., 2009; Wijesekera et al., 1998~~). The SLD emerges during the southwest monsoon. Its western branch is responsible for the observed southward flow along the eastern coast of Sri Lanka in that season (Figure 2d-f, Figure 3). During boreal fall, the surface current is northward. Similarly, northward surface flow was also observed in mooring measurements in the southern BoB in late July of 2015 at 85.5° E (Wijesekera et al., 2016b). During the winter, the southward-flowing EICC extends from the Indian east coast to the southern tip of Sri Lanka (Schott et al., 1994; Wijesekera et al, 2015) resulting in strong southward flow at 8° N (Figure 3).

3.2.2 Subsurface circulation

~~2015; Lee et al., 2016).~~ An undercurrent flowing in the opposing direction to the surface current is a prominent and consistent feature among the observations and OGCMs in boreal spring (~~March-April) and summer (June-July).~~beginning of February to mid-April) and summer (beginning of June to mid-August) (Figure 3). In boreal spring, the southward-flowing undercurrent extends from approximately 200 to 900 m depth with a velocity maximum core in the range of 300-600 m depth. The velocities derived from hydrography and Argo profiles and glider measurements confirm the existence of the undercurrent below 150-250 m, although the magnitudes are not consistent (Figure 3). This may be due to interannual variation in intensity and position of the subsurface reversed flow, combined with the sporadic sampling of the hydrography and Argo data.

~~The mean meridional surface current is~~ During the southwest monsoon, the northward ~~with speeds exceeding 10 cm s^{-1} during boreal spring (Figure 3) in good agreement with that derived from the satellite altimetry (Lee et al., 2016). The westward~~ flowing ~~North Equatorial Current is dominant at the surface in this season; it often bifurcates at the east coast of Sri Lanka splitting into a northward and~~

~~southwestward branch at approximately 7.5° N resulting in a northward surface current along the east coast (Shetye et al., 1993; Hacker et al., 1998; de Vos et al., 2014). The velocity derived from CTD and Argo profiles and glider measurements confirm the existence of the~~ undercurrent ~~below 150 m (Figure 3a,b). The southward-flowing undercurrent is the strongest during March-April. Mean velocity profiles derived from the~~is apparent in both observations and the OGCMs ~~agree that the core of the undercurrent is between 300-400~~(Figure 3). The undercurrent starts developing in May and reaches its maximum speed in June. The OGCMs also suggest an upward phase propagation during summer and early fall (May- October) with a speed of approximately 1.5 m day^{-1} in the upper 200 m ~~depth. The CTD and Argo-derived velocity shows that the mean undercurrent can reach nearly 50 cm s^{-1} at 300~~of the water column (Figure 3c, d). This feature is also evident in the geostrophic velocity derived from hydrography-Argo profiles in the upper 100 m~~. At 729 m depth, the~~ of the water column (Figure 3a).

To gain a better understanding of the subsurface circulation, we examine the POP velocity fields ~~show a~~ at 729 m (Movie S1), which encompasses the depth location of the undercurrent core in boreal spring and summer (Figures 2, 3; Tables 1, 2). In March, the undercurrent is strong and confined ~~southward undercurrent~~ to 82.5° E along the entire Sri Lankan east coast (Movie S1). ~~Figure 4a shows a simplified schematic of the~~The undercurrent ~~during boreal spring that~~ usually turns eastward around 6° N to combine with an eastward-flowing current along the Sri Lankan south coast ~~from~~, as shown in the simplified schematic derived from the ~~AS.~~POP 729 m velocity fields (Figure 4a). However, in some years (e.g. 1995, 1999, 2005, and 2007), the undercurrent turns westward around the southern ~~tip~~coast of Sri Lanka and forms a narrow current, about 50-70 km wide, on the northern side of the eastward flow (Movie S1~~).~~

~~During the boreal summer, the surface current, which forms as a western branch of the SLD, is southward and has a mean speed as high as 40 cm s^{-1}, while the northward-flowing undercurrent is found below approximately 200 m (~~; Figure ~~3). The observations and OGCMs agree~~4a). Note that ~~the undercurrent starts developing~~a similar circulation is observed in ~~May and reaches a maximum speed during June-July with a core at 800 m. The maximum mean speed can be as strong as 35 cm s^{-1} (Figure 3). In early summer,~~ the POP velocity fields ~~show~~at 318 m in March, albeit the flow is stronger. In boreal summer, there is a convergence of the eastward-flowing current along the south coast of Sri Lanka and a ~~southwestward~~westward-flowing current in the ~~southeast~~southwestern BoB at approximately 7° N ~~and~~, 82.25° E ~~as~~(Movie S1), which is also shown in ~~a~~the simplified schematic (Figure 4b). Both OGCMs agree that the convergence produces the undercurrent flowing north along the east coast of Sri Lanka that injects relatively saline water into the BoB. ~~Also~~In addition, an anticyclonic eddy ~~usually~~often develops along the east coast, trapping local saline water inside, which is then propagated northward with the eddy (Movie S1).

~~The glider-derived velocity over the 2014-2016 period shows strong northward~~ During boreal fall (mid-August to end of October) and ~~southward~~winter (beginning of November to end of January), flows in the ~~surface and~~ subsurface ~~layers during boreal fall (Figure 3b); the~~ layer are less consistent between the observations and the OGCMs (Figure 3). The models suggest that the subsurface current ~~can reach 20 cm s^{-1} at 1000 m. However, this feature might~~ is not ~~be~~ persistent across the years~~; the velocity profiles~~

~~derived from the OGCMs and the CTD and Argo profiles show a weak northward-flowing surface current and a weak southward-flowing subsurface current during boreal~~ during fall ~~(Figure 3a,c,d). The subsurface current has a maximum mean speed of 5-10 cm s^{-1} at 500-750 m depth, according to the CTD and Argo-derived velocity and the OGCMs. Standard deviation of meridional velocity across 8° N during fall derived from HYCOM and CTD and Argo profiles (9.4 cm s^{-1} and 54 cm s^{-1}) is higher than the mean (-6.8 cm s^{-1} and -11 cm s^{-1}) over the 200-1000 m layer. Also, longitude~~and winter (Movie S1). Longitude-depth transects of meridional velocity across 8° N ~~in boreal fall~~ from POP and HYCOM (not shown) do not show a well-defined undercurrent near the east coast of Sri Lanka in the top 1000 m of the water column during these seasons.

~~During boreal winter, the surface flow is southward and stronger than 40 cm s^{-1} (Figure 3). The seasonal mean subsurface current derived from CTD and Argo profiles is northward in contrast to that derived from the OGCMs and the gliders; the disagreement might arise from the small number of CTD and Argo profiles used in the velocity calculation during boreal winter (Figure 1b). The glider-derived velocity of the subsurface current is much stronger than that from the OGCMs. Since glider measurements cover the period of 2014-2016, the inconsistency suggests high variability of the subsurface current from year to year. The CTD-and-Argo-derived and the HYCOM velocity profiles also suggest that the interannual variation of the subsurface current is high; the standard deviation of the velocity below 200 m across 8°N (56 cm s^{-1} and 8.1 cm s^{-1}) is roughly twice as large as its mean (17 cm s^{-1} and -4.2 cm s^{-1}) during the winter. Moreover, the current at 729 m in the POP winter velocity fields appears as a transient current rather than a seasonal undercurrent (Movie S1). More observations are needed to understand the vertical structure and the associated dynamics of the subsurface boundary current during the winter.~~

3.3 Depth-integrated volume transport

Monthly volume transports computed from the OGCMs and volume transport computed from the discrete glider sections (referenced to depth-average velocity; e.g. Figure 2) across the 8° N transect between the eastern coast of Sri Lanka and 82.5° E (Figure 1a) over the upper (0-200 m) and lower (200-1000 m) layers are presented in Figure 5. The seasonal variation from HYCOM, POP, and glider measurements agree well, especially in the subsurface layer. Mean volume transport in the upper layer (0-200 m) has a semi-annual cycle that ranges from 1 to 6 Sv into and out of the BoB (Figure 5a). Southward flows are observed in the surface layer during boreal summer and winter. The flows are weakly northward during boreal spring and fall.

Depth-integrated transport in the subsurface layer is southward throughout the year except during the summer when the northward-flowing undercurrent is present (Figures 3, 5b). The undercurrent transport is approximately 5-7 Sv out of and 3-11 Sv into the BoB during boreal spring and summer, respectively (Table 3). Moreover, the OGCMs suggest only a small mean volume transport of the subsurface current during fall and winter compared to its standard deviation (Figure 5b) implying that the fall and winter undercurrent is not well defined in these seasons and indeed can flow northward in some years. Volume transport over the 0-1000 m layer ranges from -12 to 5 Sv and exhibits an annual cycle similar to that in the lower (200-1000 m) layer (Figure 5c).

4 Discussion

~~The undercurrent potentially plays an important role in salt and mass exchange between the AS and the BoB as suggested by the velocity fields of the OGCM. During the summer, the undercurrent injects relatively saline water into the western boundary of the BoB that can be trapped in a northward-propagating seasonal anticyclonic eddy (Figure 4b and Movie S1). Relatively freshwater is transported southward along the east coast of Sri Lanka in the subsurface layer in spring (Figure 4a). It can be advected westward along the Sri Lankan south coast in some years depending on the strength and location of the eastward flowing current along the south coast (Movie S1). The POP velocity fields further reveal that the zonal current along the south coast of Sri Lanka is the strongest during the boreal spring, early summer, and fall coinciding with the active period of the Wyrtki Jet, a surface-intensified eastward-flowing current observed in the equatorial Indian Ocean during the monsoon transitions (Wyrtki, 1973). Previous mooring measurements show that the Wyrtki jet can extend to greater than 900 m depth and reach northward beyond 5° N (Reppin et al., 1999).~~

~~The mechanisms driving the undercurrent are still unclear, but they are likely to vary at different times of the year. A Hovmöller diagram of POP meridional velocity across 8° N (Figure 5~~The circulation in the southern BoB is complex as it is controlled by various forcings, such as local winds, Ekman pumping, and equatorial waves, which impact the region in different seasons. The mechanisms driving the undercurrent remain unclear and although beyond the scope of this study we put forward some informed hypotheses based on previous studies and our observations. The Rossby waves, equatorial waves, and Ekman pumping are likely to be important for producing the undercurrent: a Hovmöller diagram of POP meridional velocity across 8° N (Figure 6) shows the westward propagation of the velocity signal at 729 m depth originating from the eastern boundary of the BoB that takes about four months to cross the southern BoB. ~~This provides~~It has a propagation speed of 12 cm s^{-1} ~~which is~~ in good agreement with the phase speed of a mode 2 baroclinic Rossby wave in this region (Shankar et al., 1996; Killworth and Blundell, 2003~~).~~; Wijesekera et al., 2016a). A westward-propagating ~~southward current begins to develop~~signal first develops at the eastern boundary of the BoB in April-May ~~and~~at the same time that the Wyrtki Jet, a surface-intensified eastward-flowing current observed in the equatorial Indian Ocean during the monsoon transitions (Wyrtki, 1973), reaches this eastern boundary. The westward-propagating signal reaches the east coast of Sri Lanka in September contributing to the ~~observed~~ southward-flowing subsurface current (~~Figure~~Figures 3 ~~and Figure 5~~); this is consistent with findings from ~~a stratified linear model~~the LSM study (McCreary et al., 1996). ~~Even though the Rossby waves do not directly influence the undercurrent observed during spring and summer, it might be important in setting up the spring undercurrent; the influence of Rossby waves on the undercurrent is still unclear and more studies are needed. The westward propagating northward and southward~~In April, the westward propagating meridional flows originating at 83° E-85° E ~~in April~~ (Figure ~~5b~~6b) are associated with the subsurface anticyclonic eddy observed along the east coast of Sri Lanka during the summer (Figure 4b). The influence of equatorial waves on the undercurrent is still unclear and more studies are needed. Upward phase propagation is present during summer and early fall (Figure 3) implying the influence of equatorial waves on the subsurface flow during this time (Luyten and

Roemmick, 1982). Equatorial waves are also known to impact currents along the Indian east coast (Mukherjee et al., 2014) and Sri Lankan south coast (Schott et al., 1994; Shankar et al., 2002).

~~The stratified linear model study~~ Ekman pumping can also significantly impact the circulation along the eastern coast of Sri Lanka (McCreary et al., 1996~~) also indicates the role of Ekman pumping in producing the undercurrent. The model suggests~~ ; Vinayachandran et al., 1999). The LSM study of McCreary et al. (1996) suggested that Ekman pumping ~~induces~~drives the undercurrent ~~during the boreal spring and summer; the~~east of Sri Lanka from April to December. The model undercurrent ~~with its~~has a core at 400-500 m that can reach a maximum speed of 10 cm s^{-1} southward and northward in March-April and August, respectively. ~~This~~ Although this value agrees quite well with that of the spring undercurrent observed in the observations and OGCMs ~~(Figure 3).~~, the magnitude given by the LSM during the summer is about half that shown in this study (Figure 3). During the winter, the mean subsurface current of the observations and OGCMS agrees with the results from the LSM (McCreary et al., 1996) within one standard deviation. This implies that a combination of local alongshore winds, Ekman pumping, and equatorial waves, which are the main mechanisms driving the subsurface current during the winter in the LSM, is important in producing the subsurface current in only some years.

~~To estimate the role of the undercurrent in the exchange of salt between the BoB and the rest of the northern Indian Ocean basin, we calculated the salt transport resulting from the reversing undercurrent.~~Circulation in the subsurface layer along the Sri Lankan east coast is characterized by reversed flows relative to the surface during boreal spring and summer similar to the subsurface circulation along the Indian east coast and Sri Lankan south coast described by previous studies (Schott et al., 1994; McCreary et al., 1996; Mukherjee et al., 2014). During the southwest monsoon, the current along the Sri Lankan south coast (Schott et al., 1994), Sri Lankan east coast (Figure 2d-f; Table 2), and Indian east coast (Mukherjee et al., 2014) reverses its direction below approximately 100-150 m. The subsurface current flows eastward along the southern coast of Sri Lanka (Schott et al., 1994) in agreement with the circulation pattern derived from the POP velocity fields (Figure 4b) and poleward along the Sri Lankan and the Indian east coast (McCreary et al., 1996; Mukherjee et al., 2014). This suggests the possibility of a subsurface conduit connecting the region off the Sri Lankan south coast to the northern BoB. However, the subsurface poleward current along the Indian east coast is not always apparent (Mukherjee et al., 2014), although it is also possible that the undercurrent during this season occurs below the deepest measurement at 300 m from the Mukherjee et al. (2014) study. In boreal spring, mooring measurements along the Sri Lankan south coast (Schott et al., 1994) verifies the existence of the eastward-flowing subsurface current observed in the POP velocity fields (Figure 4a). The subsurface current extends from approximately 250 m to 1010 m (Schott et al., 1994). Unlike the summer subsurface circulation, flow at and north of 12° N is poleward over 0-300 m (Mukherjee et al., 2014), in the opposite direction to the undercurrent off the Sri Lankan east coast (Figures 2a-c, 3). However, since the core location of the spring undercurrent is highly variable from year to year, direct velocity measurements in the deeper layer would help to gain a better understanding of the pathways of the subsurface circulation along the western boundary of the BoB during boreal spring.

Although velocity and salinity fields from POP suggest the possibility of significant salt exchange between the AS and the BoB, the estimated salt transport via the undercurrent is small based on the data and models we have available. POP velocity fields show that the summer undercurrent injects relatively saline water into the western boundary of the BoB that can be trapped in a northward-propagating seasonal anticyclonic eddy (Figure 4b). The source of the saline water is mostly from the southwest of Sri Lanka, although sometimes, such as in 1998, it originates from the eastern BoB (Movie S1). Relatively fresher water is transported southward along the east coast of Sri Lanka in the subsurface layer in spring (Figures 4a, 7). It can be advected westward along the Sri Lankan south coast in some years depending on the strength and location of the deep eastward-flowing Wyrtki jet (Reppin et al., 1999; Movie S1). The time series of salinity averaged over the width of the undercurrent (from the east coast of Sri Lanka to 82.5° E) ~~from POP~~ and the volume transport of the POP undercurrent (over 200-1000 m) along 8° N ~~are shown in Fig. 6. The time series~~ clearly ~~shows fresh~~show a positive correlation *i.e.* the undercurrent tends to export freshwater from the BoB and import saline water ~~flowing southward and salty~~into the BoB (Figure 7). The hydrography-Argo profiles, glider measurements, and HYCOM also show that poleward subsurface transport is associated with relatively saline water ~~flowing northward with a~~ and vice versa (not shown). The correlation coefficient ~~of~~between the subsurface transport and salinity computed from POP is 0.50 ~~that is,~~ significant at the 95% confidence level. The salt ~~transport~~flux due to the fluctuations of the flow and of the salinity (departures from the 13-year climatology) in the 200-1000 m layer from POP is 0.04×10^6 kg s^{-1}. ~~This~~ (Figure 7), while the estimated salt flux from the hydrography-Argo profiles and glider measurements are 0.19×10^6 and 0.09×10^6 kg s^{-1}, respectively. The difference between the observational and POP salt fluxes arises from the smaller salinity range of the model compared to the observations (Table 3). The estimated salt input is ~~only 1~~up to 4% of the total expected salt transport into the BoB of $4.5\text{-}4.9\times10^6$ kg s^{-1}, which is estimated from ~~an expected~~the annual freshwater input of 0.13-0.14 Sv (Rao and Sivakumar, 2003; Sengupta et al., 2006; Wilson and Riser, 2016). Note that the total net salt transported ~~in~~by POP into the BoB across 8° N is 4.3×10^6 kg s^{-1} ~~which~~; this value is in good agreement with the ~~previously reported values~~expected salt transport discussed above. Estimates of salt flux by the *mean* flow over the same depth layer from POP and HYCOM are even smaller: the mean undercurrent transport of 1.5-2 Sv in the OGCMs is fresher than the interior northward flow as judged from HYCOM and sparse ~~CTD~~hydrography and Argo profiles (not shown), but the salinity contrast at this depth layer is ~~very small~~smaller than 0.01. In addition, the small salt transport from the mean flow in the 200-1000 m layer might be due to the core of the undercurrent moving vertically such that this layer may sometimes include opposite flows or smaller salinity contrasts with the interior (~~Figure 3~~Figures 2, 3; Table 1, 2).

~~Compared to observations of other low-latitude western boundary undercurrents, e.g. the Mindanao Undercurrent (MUC) in the Pacific Ocean, the undercurrent along the east coast of Sri Lanka exhibits many similar physical properties. Both undercurrents span over 400 m to a depth greater than 1000 m. The MUC core is located between 500-950 m with a maximum mean speed of 10-20 cm s^{-1} (Hu et al., 1991; Zhang et al., 2014) and the undercurrent along the Sri Lankan east coast has its core between 300-800 m with a maximum mean speed of 15-30 cm s^{-1} (Figure 3). However, the MUC is narrower, about 50 km wide. Also, the MUC does not exhibit distinct seasonal variation (Qu et al., 2012; Hu et al., 2016), while the undercurrent along the Sri Lankan east coast reverses its direction seasonally. Both~~

~~Ekman pumping and Rossby waves are important in modifying the MUC (Qu et al., 2012; Chiang and Qu, 2013; Zhang et al., 2014; Hu et al., 2016). While Ekman pumping is likely to have significant impact on the undercurrent along the Sri Lankan east coast, the role of Rossby waves is still unclear.~~ An alternative interbasin-exchange pathway is through the interior of the BoB, particularly during the southwest and northeast monsoon (Vinayachandran et al., 1999; Wijesekera et al., 2015; Wijesekera et al., 2016b). Observations indicate that the eastward-flowing southwest monsoon current (SMC) has a role in the injection of saline water originating in the AS into the southern central BoB during early summer. As the summer progresses, the seasonal cyclonic (*i.e.* the SLD) and anticyclonic eddies influence the pathway of the SMC (Vinayachandran and Yamagata, 1997; Vinayachandran et al., 1999). Mooring observations at 85.5° E from 5° N to 8° N reveal a northward-flowing subsurface SMC that is associated with high salinity water (Wijesekera et al., 2016a; Wijesekera et al., 2016b). During the northwest monsoon, mass and salt exchange between the AS and the BoB is also observed in the interior over the 50-75 m layer in the southern BoB, approximately between 82.5° E and 85° E (Wijesekera et al., 2015).

5 Summary

The velocity fields derived from ~~CTD~~hydrography and Argo profiles, glider measurements, POP, and HYCOM reveal the presence of an undercurrent off the east coast of Sri Lanka ~~that reverses~~ during boreal spring and summer, which has opposite direction to the seasonally~~.~~ reversing surface flow. The ~~OGCMs also suggest active salt transport along the east coast~~location and width of ~~Sri Lanka by~~ the core of the undercurrent~~. Salt transport across 8° N by the fluctuating~~ change seasonally. The undercurrent ~~estimated from POP contributes about 1%, and~~ shows the ~~transport by~~greatest interannual variability during spring, which is likely due to the ~~mean~~ influence of El Niño events. The observations and OGCMs suggest that the undercurrent ~~estimated from HYCOM is under 0.1% of the expected total salt input into~~over the ~~BoB~~200-1000 m layer transports more water than the surface current over the 0-200 m layer. The mechanisms driving the undercurrent are still unclear, though Ekman pumping is likely to affect the undercurrent especially during the boreal spring (McCreary et al., 1996~~).~~.; Vinayachandran et al., 1999). Upward phase propagation is distinct during the summer suggesting the influence of equatorial forcing on the circulation across 8° N. Our analyses do not observe the direct influence of Rossby waves on the modification of the spring and summer undercurrent~~, but they might have~~. Although the POP velocity fields suggest a ~~crucial role in setting up the southward-flowing spring~~potential pathway in salt exchange between the AS and the BoB, salt transport across 8° N by the undercurrent~~. Understanding the role and driving~~ estimated from POP and the observations is expected to be less than 4% of the total salt input into the BoB required to balance the freshwater sources. More studies are needed to determine the mechanisms ~~of~~driving the undercurrent ~~can potentially, in~~and its role in interbasin salt and mass exchange. In turn, ~~provide~~this knowledge will lead to a better understanding of ~~what drives the contrasting salinity distribution~~property exchanges in the northern Indian Ocean.

Acknowledgements

This work is supported by the US Office of Naval Research (ONR) as part of two ONR Departmental Research Initiatives: Air-Sea Interactions Regional Initiative (ASIRI) and Northern Arabian Sea Circulation – autonomous research (NASCar) projects through ONR grants N00014-14-1-0629 (A. Anutaliya and U. Send), N00014-15-1-2189 (J. L. McClean), N00014-16-1-2313 (J. Sprintall), N00014-13-1-0478, N00014-15-1-2296, N00014-15-1-2231 (L. Rainville and C. Lee). J. Metzger and A. Wallcraft are supported by the "Eddy resolving global ocean prediction including tides" project under ONR program element 0602435N. ~~CTD~~Hydrographic profiles are from the National Center of Environmental Information (Boyer et al., 2013) (https://www.nodc.noaa.gov/access/index.html). Argo data were collected and made freely available by the International Argo Program and the national programs that contribute to it (http://www.argo.ucsd.edu, http://argo.jcommops.org). The Argo Program is part of the Global Ocean Observing System. The altimeter products were produced by Ssalto/Duacs and distributed Aviso, with support from Cnes (http://www.aviso.altimetry.fr/duacs/). The HYCOM simulation was performed using grants of computer time from the Department of Defense High Performance Computing Modernization Program. This is NRL contribution NRL/JA/7320-17-3395, which is approved for public release and distribution is unlimited. The POP simulation was carried out using the Extreme Science and Engineering Discovery Environment (XSEDE), which is supported by National Science Foundation grant number ACI-1548562. POP output is available from XSEDE. Thanks to He Wang (SIO) for helpful discussions about the salt transport calculation. Also, thanks to Judy Gaukel (SIO) for extracting and transferring the OGCM files.

References

Boyer, T.P., J. I. Antonov, O. K. Baranova, C. Coleman, H. E. Garcia, A. Grodsky, D. R. Johnson, R. A. Locarnini, A. V. Mishonov, T.D. O'Brien, C.R. Paver, J.R. Reagan, D. Seidov, I. V. Smolyar, and M. M. Zweng, (2013), World Ocean Database 2013, NOAA Atlas NESDIS 72, S. Levitus, Ed., A. Mishonov, Technical Ed.; Silver Spring, MD, 209 pp., http://doi.org/10.7289/V5NZ85MT

~~Chiang, T. L., and T. Qu (2013), Subthermocline eddies in the western equatorial Pacific as shown by an eddy-resolving OGCM. J. Phys. Oceanogr., 43, 1,241-1,253, doi:10.1175/JPO-D-12-0187.1.~~

de Vos, A., C. B. Pattiaratchi, and E. M. S. Wijeratne (2014), Surface circulation and upwelling patterns around Sri Lanka. Biogeosciences, 11, 5,905-5,930. doi:10.5194/bg-11-5909-2014.

Delman, S. A., J. L. McClean, J. Sprintall, L. D. Talley, E. Yulaeva, and S. R. Jayne (2015), Effects of Eddy Vorticity Forcing on the Mean State of the Kuroshio Extension. J. Phys. Oceanogr., 45, 1,356–1,375.

Ducet, N., P. Y. L. Traon, and G. Reverdin (2000), Global high-resolution mapping of ocean circulation from TOPEX/Poseidon and ERS-1 and -2. J. Geophys. Res., 105, 19,477-19,498.

Durand, F., D. Shankar, F. Birol, and S. S. C. Shenoi (2009), Spatiotemporal structure of the East India Coastal Current from satellite altimetry. J. Geophys. Res., 114, C02013, doi:10.1029/2008JC004807.

Eigenheer, A., and D. Quadfasel (2002), Seasonal variability of the Bay of Bengal circulation inferred from TOPEX/Poseidon altimetry. J. Geophys. Res., 105, 3,243-3,252, doi:10.1029/1999JC900291.

Gordon, A. L., E. L. Shroyer, A. Mahadevan, D. Sengupta, and M. Freilich (2016), Bay of Bengal: 2013 northeast monsoon upper-ocean circulation. Oceanography, 29(2), 82-91, http://dx.doi.org/10.5670/oceanog.2016.41.

Hacker, P., E. Firing, and J. Hummon (1998), Bay of Bengal currents during the northeast monsoon. Geophys. Res. Lett., 25(15), 2,769-2,772, doi:10.1029/98GL52115.

Hu, D., M. Cui, T. Qu, and Y. Li (1991), A subsurface northward current off Mindanao identified by dynamic calculation. Oceanogr. Asian Marginal Seas-Elsevier Oceanogr. Ser., 54, 359-365, doi:10.1016/S0422-9894(08)70108-9.

Hu, S., D. Hu, C. Guan, F. Wang, L. Zhang, F. Wang, and Q. Wang (2016), Interannual Variability of the Mindanao Current/ Undercurrent in Direct Observations and Numerical Simulations. J. Phys. Oceanogr., 46, 483-499.

Jensen, T.G., H. W. Wijesekera, E. S. Nyadjro, P. G. Thoppil, J. F. Shriver, K. K. Sandeep, and V. Pant (2016), Modeling salinity exchanges between the equatorial Indian Ocean and the Bay of Bengal. Oceanography, 29(2), 92-101, http://dx.doi.org/10.5670/oceanog.2016.42.

Killworth, P. D., and J. R. Blundell (2003), Long extratropical planetary wave propagation in the presence of slowly varying mean flow and bottom topography. Part I: The local problem. J. Phys. Oceanogr., 33, 784-801.

Lee, C. M., S. U. P. Jinadasa, A. Anutaliya, L. R. Centurioni, H. J. S. Fernando, V. Hormann, M. Lankhorst, L. Rainville, U. Send, and H. W. Wijesekera (2016), Collaborative observations of boundary currents, water mass variability, and monsoon response in the southern Bay of Bengal. Oceanography, 29(2), 102–111, http://dx.doi.org/10.5670/oceanog.2016.43.

Luyten, J. R., and D. H. Roemmick (1982), Equatorial currents at semiannual period in the Indian Ocean, J. Phys. Oceanogr., 12, 406-413.

Maltrud, M. E., F. O. Bryan, and S. Peacock (2010), Boundary impulse response functions in a century-long eddying global ocean simulation. Environ. Fluid Mech., 10, 275-295, doi:10.1007/s10652-009-9154-3.

McCreary, J. P., W. Han, D. Shankar, and S. R. Shetye (1996), Dynamics of the East India Coastal Current 2. Numerical solutions. J. Geophys. Res., 101, 13,993-14,010, doi:10.1029/96JC00560.

Metzger, E. J., H. E. Hurlburt, X. Xu, J. F. Shriver, A. L. Gordon, J. Sprintall, R. D. Susanto, H. M. van Aken (2010), Simulated and observed circulation in the Indonesian Seas: 1/12o global HYCOM and the INSTANT observations. Dyn. Atmos. Oceans, 50, 275-300, doi:10.1016/j.dynatmoce.2010.04.002.

Mukherjee et al., (2014), Observed seasonal and intraseasonal variability of the East India Coastal Current on the continental slope. J. Earth Syst. Sci., 123, 1,197-1,232, doi:10.1007/s12040-014-0471-7.

Maltrud, M. E., F. O. Bryan, and S. Peacock (2010), Boundary impulse response functions in a century-long eddying global ocean simulation. Environ. Fluid Mech., 10, 275-295, doi:10.1007/s10652-009-9154-3.

Qu, T., T. L. Chiang, C. R. Wu, P. Dutrieux, and D. Hu (2012), Mindanao Current/ Undercurrent in an eddy-resolving GCM. J. Geophys. Res., 117, C06026, doi:10.1029/2011JC007838.

Rao, R. R., R. Sivakumar (2003), Seasonal variability of sea surface salinity and salt budget of the mixed layer of the north Indian Ocean. J. Geophys. Res. Oceans, 108(C1), 9-1 – 9-14, doi:10.1029/2001JC00907.

Reppin, J., F. A. Schott, and J. Fischer (1999), Equatorial currents and transports in the upper central Indian Ocean: Annual cycle and interannual variability. J. Geophys. Res., 104(C7), 15,495-15,514.

Rosmond, T. E., J. Teixeira, M. Peng, T. F. Hogan, and R. Pauley (2002), Navy Operational Global Atmospheric Prediction System (NOGAPS): forcing for ocean models. Oceanography, 15(1), 99-108.

Schott, F. A., J. Reppin, and J. Fischer (1994), Currents and transports of the Monsoon Current south of Sri Lanka. J. Geophys. Res., 99 (C12), 25,127-25,141.

Sengupta, D., G. N. Bhsrath Raj, S. S. C. Shenoi (2006), Surface freshwater from Bay of Bengal runoff and Indonesian Throughflow in the tropical Indian Ocean. Geophys. Res. Lett., 33(22), L22609, doi:10.1029/2006GL027573.

Shankar, D., J. P. McCreary, and W. Han (1996), Dynamics of the East India Coastal Current 1. Analytic solutions forced by interior Ekman pumping and local alongshore winds. J. Geophys. Res., 101(C6), 13,975-13,991.

Shankar, D., P. N. Vinayachandran, and A. S. Unnikrishnan (2002), The monsoon currents in the north Indian Ocean. Prog. Oceanogr., 52, 63-120, doi:10.1016/S0079-6611(02)00024-1.

Shetye, S. R., A. D. Gouveia, S. S. C. Shenoi, D. Sundar, G. S. Michael, and G. Nampoothiri (1993), The western boundary current of the seasonal subtropical gyre in the Bay of Bengal. J. Geophys. Res., 98(C1), 945-954.

Shetye, S. R., A. D. Gouveia, D. Shankar, S. S. C. Shenoi, P. N. Vinayachandran, D. Sundar, G. S. Michael, and G. Nampoothiri (1996), Hydrography and circulation in the western Bay of Bengal during the northeast monsoon. J. Geophys. Res., 101, 14,011-14,025.

Smith, R., P. Jones, B. Briegleb, F. Bryan, G. Danabasoglu, J. Dennis, J. Dukowicz, C. Eden, B. Fox-Kemper, P. Gent, M. Hecht, S. Jayne, M. Jochum, W. Large, K. Linday, M. Maltrud, N. Norton, S. Peacock, M. Vertenstein, and S. Yeager (2010), The Parallel Ocean Program (POP) reference manual. LANL/NCAR Tech. Rep. LAUR-10-01853, 140 pp.

Vinayachandran, P. N., and T. Yamagata (1997), Monsoon response of the sea around Sri Lanka: generation of thermal domes and anticyclonic vortices. J. Phys. Oceanogr., 28, 1,946-1,960.

Vinayachandran, P. N., Y. Masumoto, T. Mikawa, and T. Yamagata (1999), Intrusion of the southwest monsoon current into the Bay of Bengal. J. Geophys. Res., 104(C5), 11,077-11,085.

Vinayachandran, P. N., D. Shankar, S. Vernekar, K. K. Sandeep, P. Amol, C. P. Neema, and A. Chatterjee (2013), A summer monsoon pump to keep the Bay of Bengal salty. Geophys. Res. Lett., 40, 1777-1782, doi:10.1002/grl.50274.

Wilson, E. A., S. C., Riser (2016), An Assessment of the Seasonal Salinity Budget for the Upper Bay of Bengal. J. Phys. Oceanogr., 46, 1,361-1,376.

Wijesekera, H. W., T. G. Jensen, E. Jarosz, W. J. Teague, E. J. Metzger, D. W. Wang, S. U. P. Jinadasa, K. Arulananthan, L.R. Centurioni, and H. J. S. Fernando (2015), Southern Bay of Bengal

currents and salinity intrusions during the northeast monsoon. J. Geophys. Res. Oceans, 120, 6,897-6,913, doi:10.1002/2015JC010744.

Wijesekera, H. W., … (2016a), Observations of currents over the deep southern Bay of Bengal – With a little luck. Oceanography. 29, 112-123, doi:10.5670/oceanog.2016.44.

Wijesekera, H. W., W. J. Teague, D. W. Wang, E. Jarosz, and T. G. Jensen (2016b), Low-Frequency Currents from Deep Moorings in the Southern Bay of Bengal. J. Phys. Oceanogr., 46, 3,209-3,238, doi: 10.1175/JPO-D-16-0113.1.

Wilson, E. A., S. C. Riser (2016), An Assessment of the Seasonal Salinity Budget for the Upper Bay of Bengal. J. Phys. Oceanogr., 46, 1,361-1,376.

Wyrtki, K. (1973), An Equatorial Jet in the Indian Ocean. Science, 181, 262-264.

Yu, L., J. J. O'Brien, and J. Yang (1991), On the Remote Forcing of the Circulation in the Bay of Bengal. J. Geophys. Res., 96, 20,449-20,454.

~~Zhang, L., D. Hu, S. Hu, F. Wang, F. Wang, and D. Yuan (2014), Mindanao Current/ Undercurrent measured by a subsurface mooring~~

Tables and Figure

	v_{max} (cm s^{-1})	Depth of v_{max} (m)	Position of v_{max} (° E)	Depth of reversal (m)	Width (km)
Glider	-25.3	1000.0	82.06	232.0	107.8
HYCOM	-16.2	570.4	82.00	83.3	151.9
POP	-18.9	268.5	81.95	77.4	209.1

Table 1. Statistics of the undercurrent across 8° N in March from the glider geostrophic velocity as presented in Figure 2 and mean absolute velocity from HYCOM and POP. Here, v_{max} represents maximum meridional velocity; depth of reversal is defined as the depth of the zero meridional velocity at the location of the maximum velocity; width of the undercurrent is defined as the distance from the coast at the depth of maximum velocity to the location where the meridional velocity is zero.

	v_{max} (cm s^{-1})	Depth of v_{max} (m)	Position of v_{max} (° E)	Depth of reversal (m)	Width (km)
Glider	29.6	1000.0	81.90-82.40	117.3-300	206.9
HYCOM	20.6	800.8	82.08	244.8	165.1
POP	27.6	918.4	82.15	244.1	172.8

Table 2. Same as Table 1 but for June.

	Mean transport (Sv)		Seasonal salinity range
	Spring	Summer	
Hydrography -Argo	-6.9	9.7	0.09
Glider	-5.7	11.42	0.04
HYCOM	-4.6	3.0	0.01

POP	-5.7	6.8	0.01

Table 3. Mean transport and seasonal salinity range of the undercurrent (200-1000 m) across 8° N in boreal spring (February to mid-April as highlighted by white lines in Figure 3) and summer (June to mid-August as highlighted by yellow lines in Figure 3) from hydrography-Argo profiles, glider measurements, HYCOM, and POP. Seasonal salinity range is the approximate difference between boreal spring and summer extremes in average seasonal cycle. Note that the statistics representing glider measurements are derived from gridded velocity referenced to its depth-averaged velocity (e.g. Figure 2) and salinity interpolated onto 8° N.

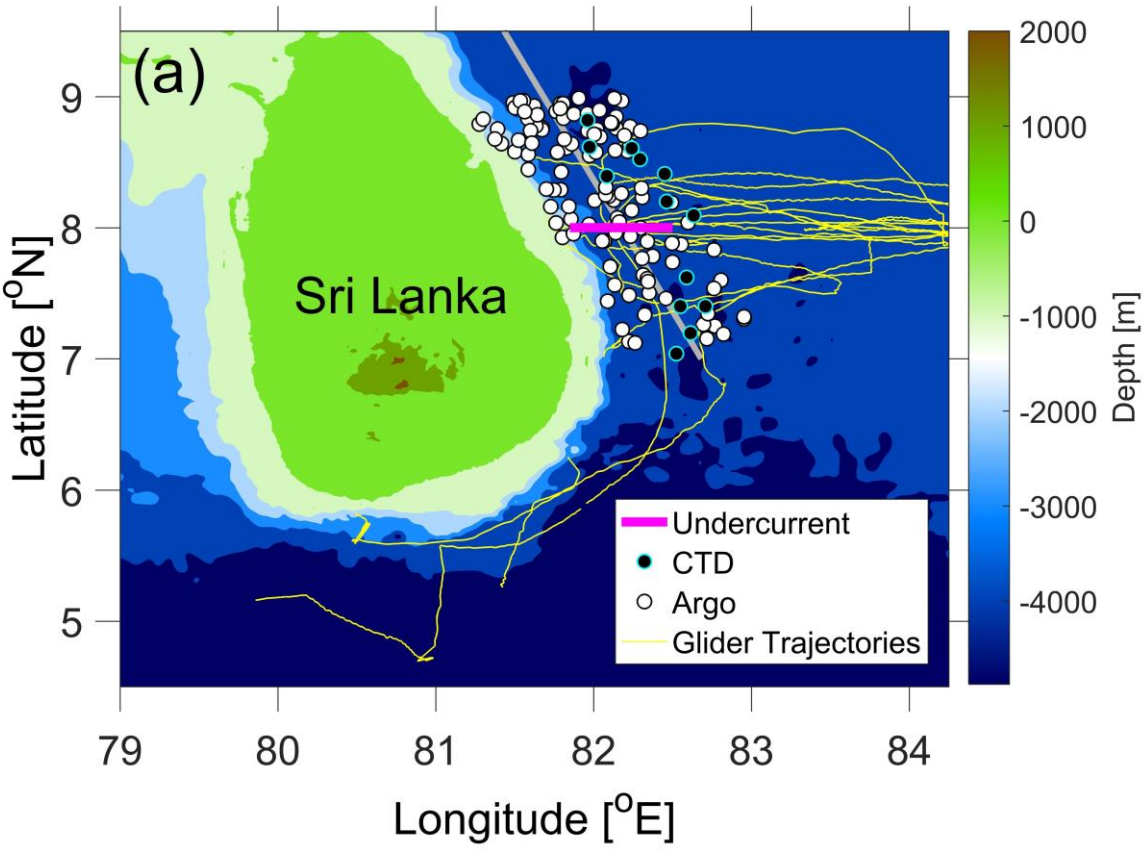

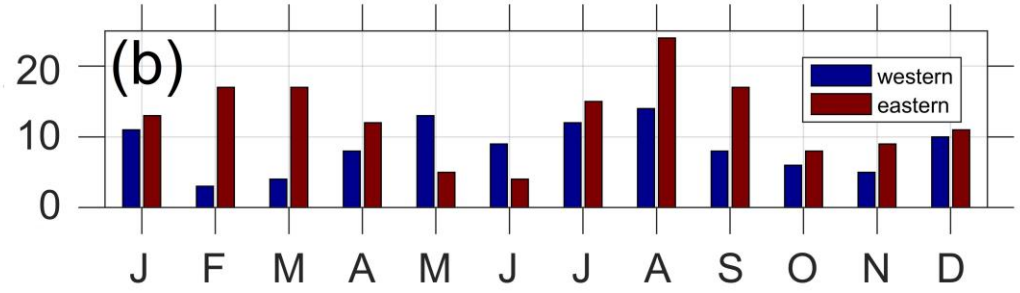

~~. J. Geophys. Res. Oceans, 119, 3,617-3,628, doi:10.1002/2013JC009693.~~

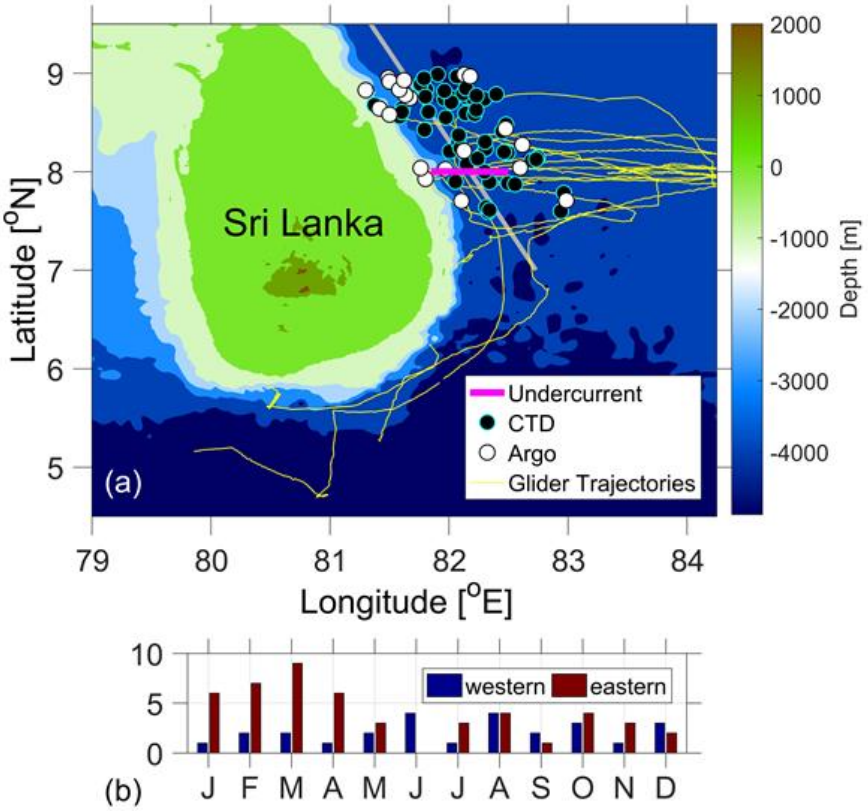

Figure 1: Bathymetry around Sri Lanka (a) with the location of the ~~CTD~~shipboard hydrography measurements (black dots), Argo profiles (white dots), and glider measurement transects (yellow lines). The ~~gray~~grey line divides ~~CTD~~hydrography and Argo measurements into the eastern and western ~~halves~~sectors used in the seasonal mean dynamic height calculation. The OGCM outputs are interpolated along 8° N (magenta line). The number of ~~CTD~~hydrography and Argo profiles available in the mean dynamic height calculation for each month for the eastern (red) and western (blue) ~~halves~~sectors are shown in (b).

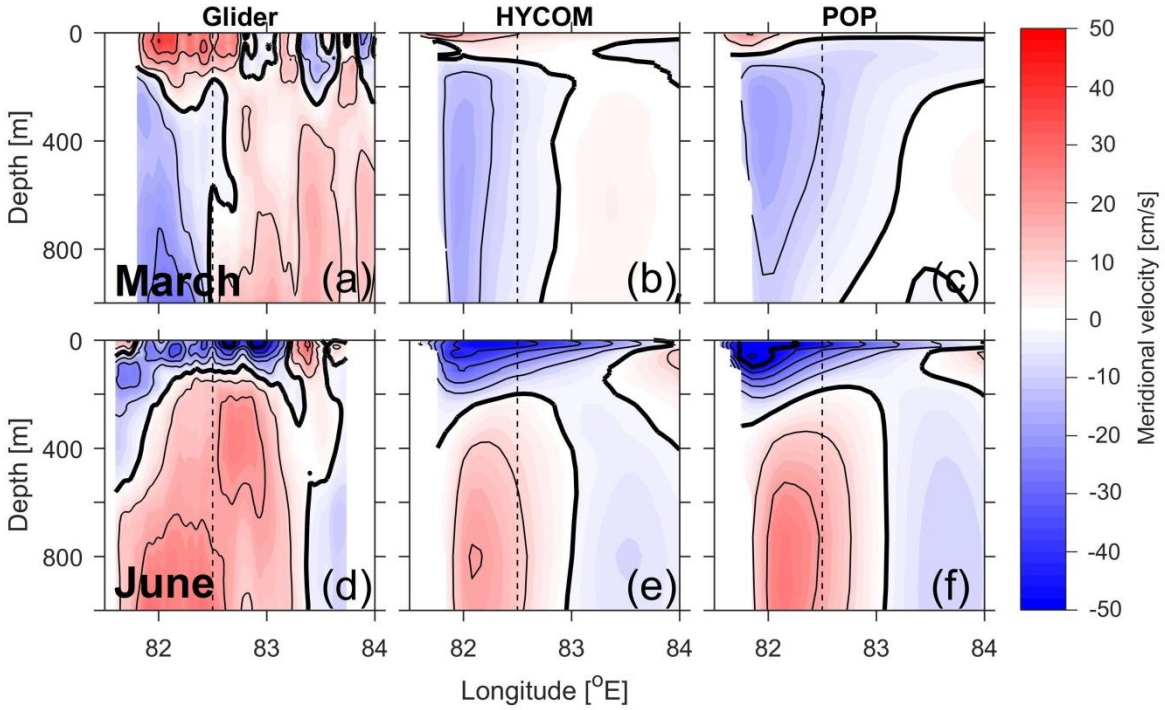

Figure 2: ~~Absolute geostrophic~~Geostrophic meridional velocity referenced to the depth-averaged velocity across 8° N ~~measured by gliders~~from glider measurements during March 18-30, 2014 (a) and May 24 – Jun 8, 2014 (d), the mean absolute meridional velocity from HYCOM (b and e) and POP (c and f) in March and June over 2003-2012 and 1995-2007 periods, respectively. The black dashed line marks the typical eastern ~~boundary~~extent of the undercurrent core; the region bounded to its west is used for a subsequent averaging in Figure 3. Thin black lines are plotted every 10 cm s^{-1}, and thick black lines are plotted every 50 cm s^{-1}.

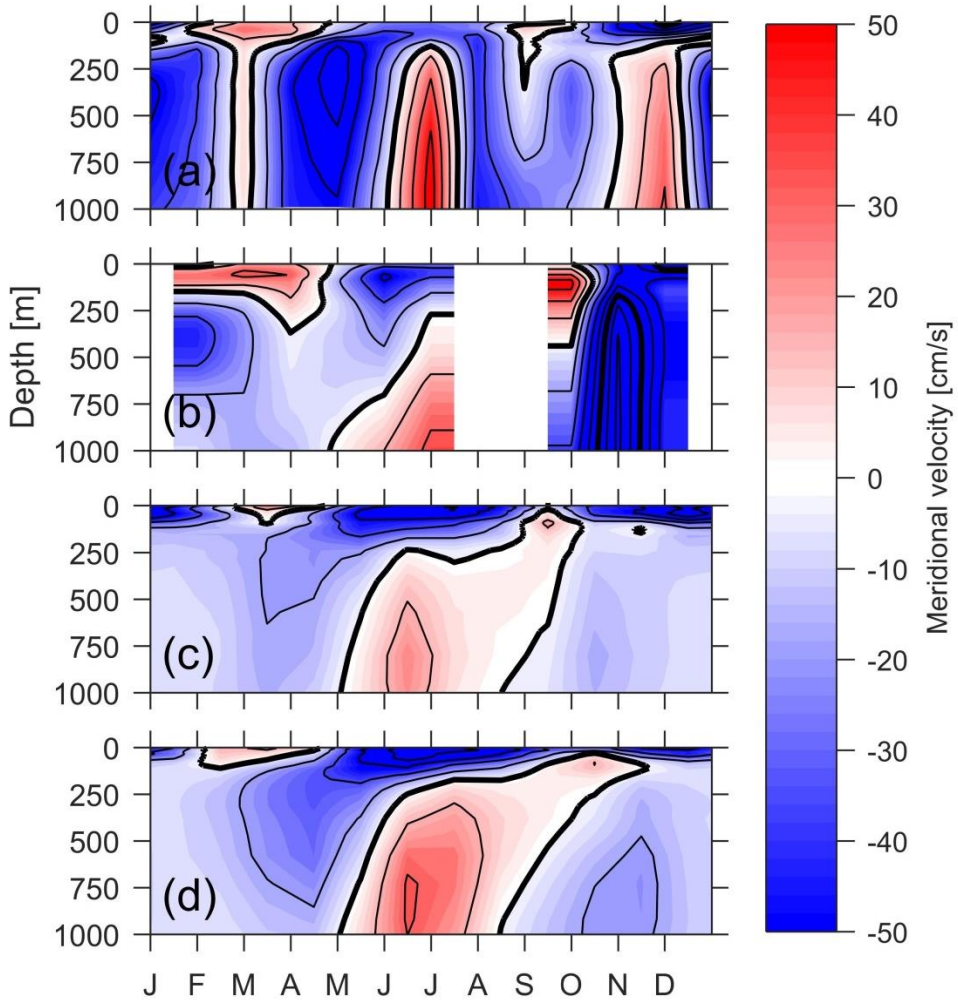
Depth [m]
0
250
500
750
1000
(a)
(b)
(c)
(d)
J F M A M J J A S O N D
Meridional velocity [cm/s]
50
40
30
20
10
0
-10
-20
-30
-40
-50

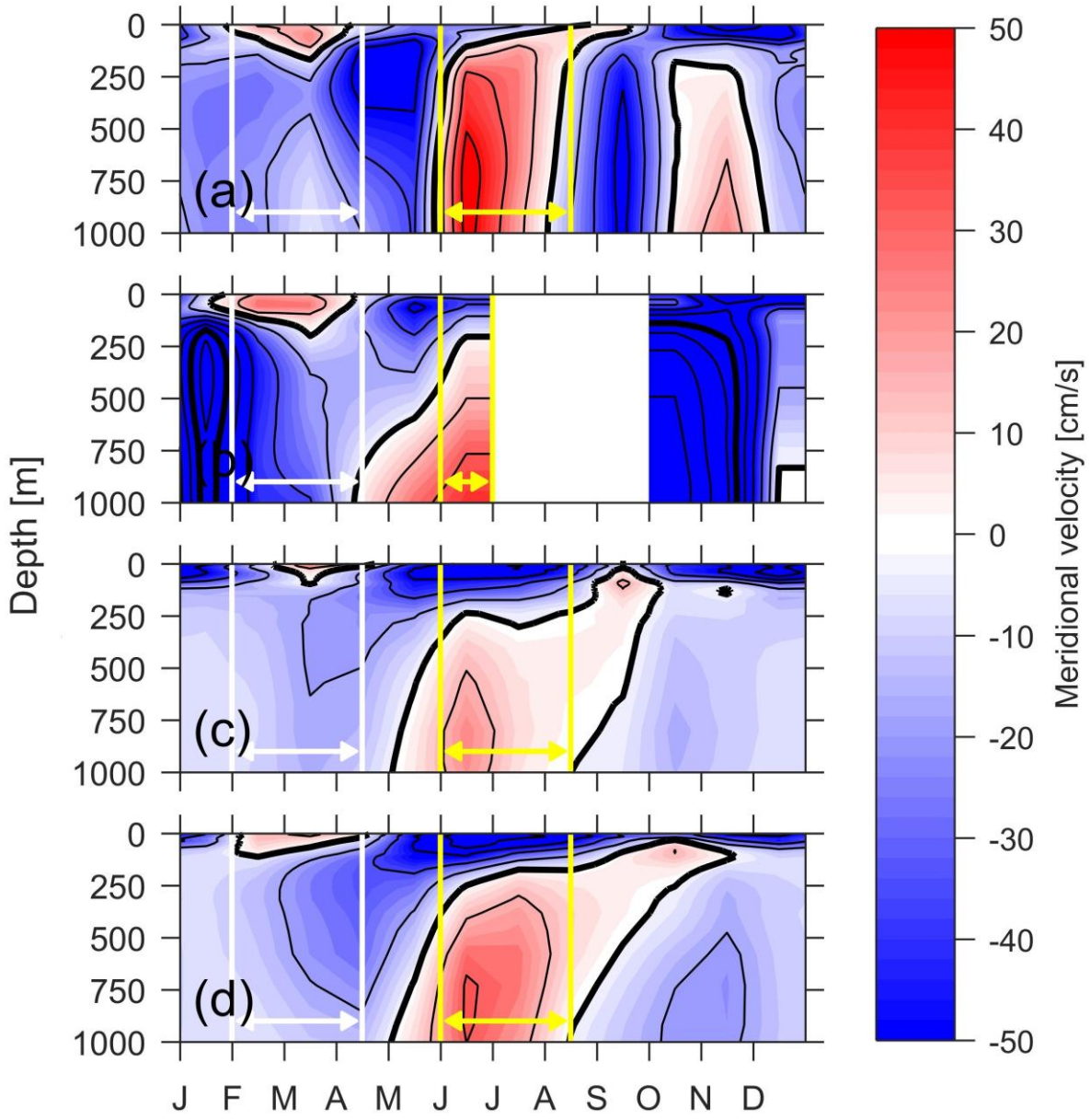

Figure 3. Bimonthly ~~sliding~~ mean seasonal variation of the meridional geostrophic velocity ~~profiles derived from CTD~~referenced to the surface satellite ADT across the magenta transect in Figure 1 from hydrography and Argo measurements (a), glider measurements (b), ~~and~~ monthly mean meridional velocity profiles ~~averaged across the magenta transect shown in Fig. 1 from~~ from HYCOM (c), and POP ~~outputs (d).~~ output. Line contours are plotted in the same manner as in ~~Fig.~~Figure 2. White and yellow lines indicate periods when the undercurrent is most pronounced.

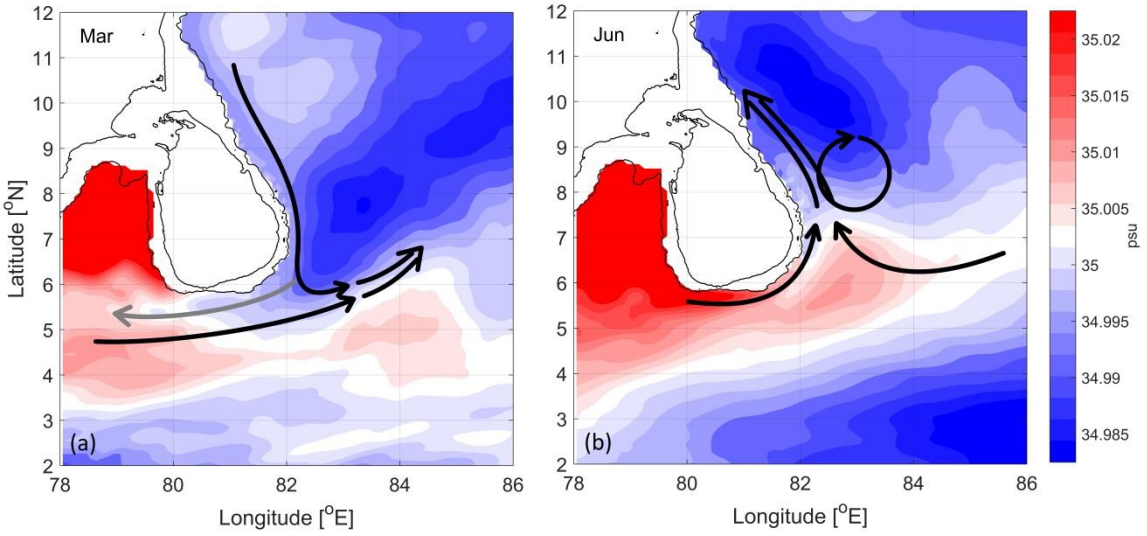

Figure 4. Simplified schematic of the undercurrent along the east and south coast of Sri Lanka at 729 m depth based on POP outputs in March (a) and June (b) plotted over the corresponding POP monthly mean salinity. The black arrows represent the annual current ~~pattern~~patterns at 729 m ~~that reoccurs every year~~, and the gray arrow shows circulation that is observed ~~only in some years~~occasionally. The 0 and 1000 m bathymetry contours are plotted as thin black lines.

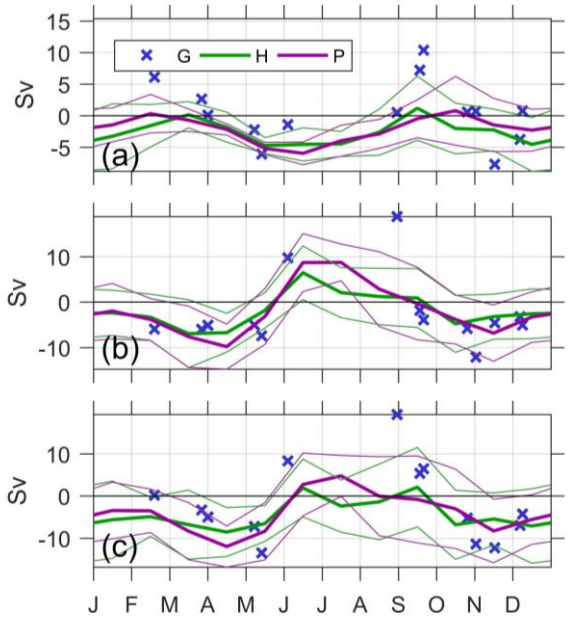

Figure 5. Meridional volume transport across 8° N from the Sri Lankan east coast to 82.5° E (dashed line in Figure 2) calculated from glider geostrophic velocity referenced to the depth-averaged velocity (G; blue cross) and absolute velocity fields from HYCOM (H; thick green line) and POP (P; thick purple line) over the 0-200 m (a), 200-1000 m (b), and 0-1000 m (c) layers. Thin lines designate the mean value +/- one standard deviation.

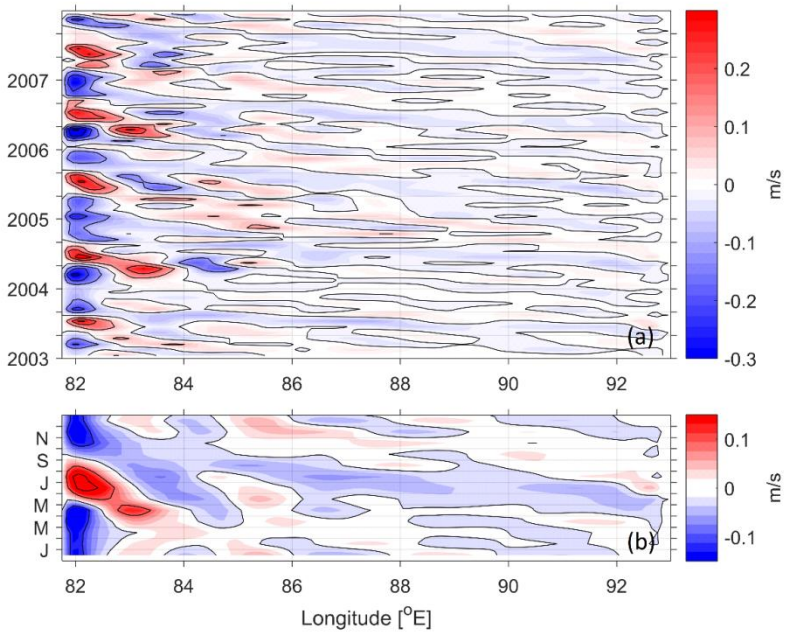

~~Figure 5.~~ **Figure 6. Time-longitude plots of monthly meridional velocity (a) and seasonal mean velocity (b) over 2003-2007 across 8° N at 729 m from POP. Note the difference in color scale.**

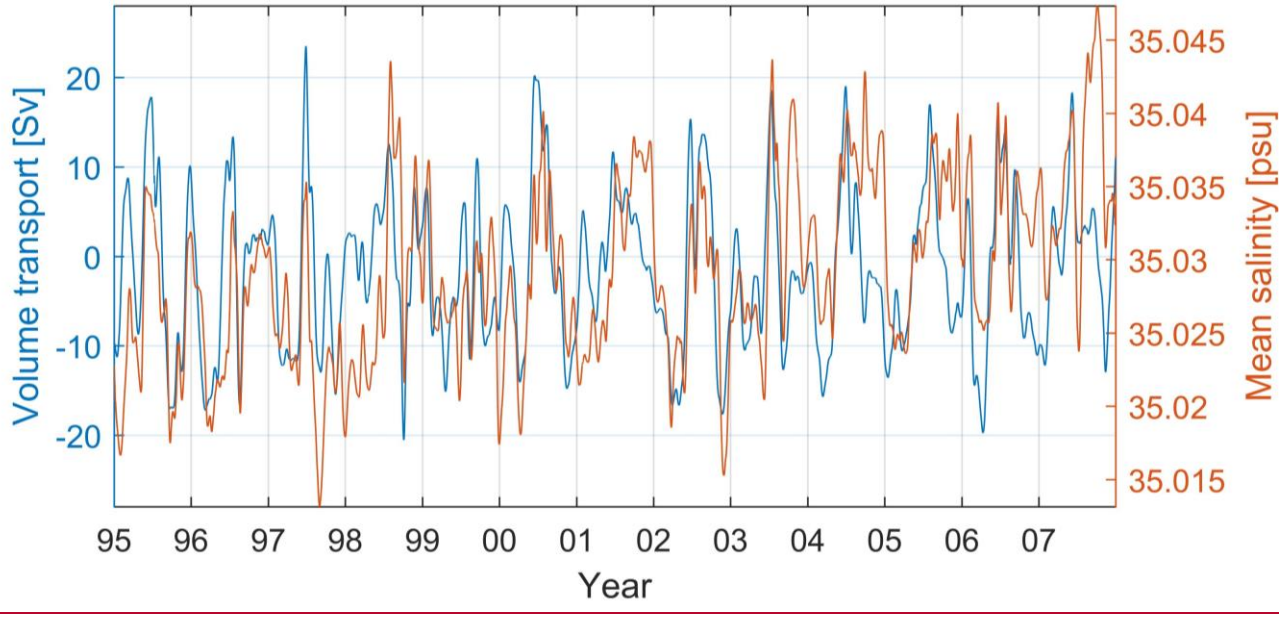

Figure ~~6~~7. Time series of volume transport (blue) and mean salinity (orange) between 81.5° E and 82.~~4~~5° E ~~in~~over the 200-1000 m layer from POP.